Dinosaur bonebed amber from an original swamp forest soil

Sergio Álvarez-Parra[1]*, Ricardo Pérez-de la Fuente[2], Enrique Peñalver[3], Eduardo Barrón[3], Luis Alcalá[4], Jordi Pérez-Cano[1], Carles Martín-Closas[1], Khaled Trabelsi[5,6,7], Nieves Meléndez[8], Rafael López Del Valle[9], Rafael P Lozano[3], David Peris[1], Ana Rodrigo[3], Víctor Sarto i Monteys[10], Carlos A Bueno-Cebollada[3], César Menor-Salván[11,12], Marc Philippe[13], Alba Sánchez-García[14,15], Constanza Peña-Kairath[1], Antonio Arillo[16], Eduardo Espílez[4], Luis Mampel[4], Xavier Delclòs[1]

[1]Departament de Dinàmica de la Terra i de l'Oceà and Institut de Recerca de la Biodiversitat (IRBio), Facultat de Ciències de la Terra, Universitat de Barcelona, c/ Martí i Franquès s/n, 08028, Barcelona, Spain.

[2]Oxford University Museum of Natural History, Parks Road, Oxford, OX1 3PW, UK.

[3]Museo Geominero (IGME, CSIC), c/ Ríos Rosas 23, 28003, Madrid, Spain.

[4]Fundación Conjunto Paleontológico de Teruel-Dinópolis/Museo Aragonés de Paleontología, Av. Sagunto s/n, 44002, Teruel, Spain.

[5]Université de Sfax, Faculté des Sciences de Sfax, 3038, Sfax, Tunisie.

[6]Université de Tunis El Manar II, Faculté des Sciences de Tunis, LR18 ES07, 2092, Tunis, Tunisie.

[7]Department of Geology, University of Vienna, UZA 2, Althanstrasse 14, 1090, Vienna, Austria.

[8]Departamento de Geodinámica, Estratigrafía y Paleontología, Facultad de Ciencias Geológicas, Universidad Complutense de Madrid, Ciudad Universitaria, 28040, Madrid, Spain.

[9]Museo de Ciencias Naturales de Álava, c/ Siervas de Jesús 24, 01001, Vitoria-Gasteiz, Spain.

[10]Institut de Ciència i Tecnologia Ambientals (ICTA), Edifici Z – ICTA-ICP, Universitat Autònoma de Barcelona, 08193, Bellaterra, Barcelona, Spain.

[11]Departamento de Biología de Sistemas/Instituto de Investigación Química "Andrés del Río" (IQAR), Universidad de Alcalá, 28805, Alcalá de Henares, Madrid, Spain.

[12]School of Chemistry and Biochemistry, Georgia Institute of Technology, Atlanta, GA 30332, USA.

[13]Univ. Lyon, Université Claude Bernard Lyon 1, CNRS, ENTPE, UMR 5023 LEHNA, F-69622, Villeurbanne, France.

[14]Departament de Botànica i Geologia, Facultat de Ciències Biològiques, Universitat de València, c/ Dr. Moliner 50, 46100, Burjassot, Valencia, Spain.

[15]Division of Invertebrate Zoology, American Museum of Natural History, Central Park West at 79th Street, New York, NY 10024-5192, USA.

[16]Departamento de Biodiversidad, Ecología y Evolución, Facultad de Biología, Universidad Complutense de Madrid, c/ José Antonio Novais 12, 28040, Madrid, Spain.

*Correspondence: sergio.alvarez-parra@ub.edu

Abstract

Dinosaur bonebeds with amber content, yet scarce, offer a superior wealth and quality of data on ancient terrestrial ecosystems. However, the preserved palaeodiversity and/or taphonomic characteristics of these exceptional localities had hitherto limited their palaeobiological potential. Here we describe the amber from the

Lower Cretaceous dinosaur bonebed of Ariño (Teruel, Spain) using a multidisciplinary approach. Amber is found in both a root layer with amber strictly in situ and a litter layer namely composed of aerial pieces unusually rich in bioinclusions, encompassing 11 insect orders, arachnids, and a few plant and vertebrate remains, including a feather. Additional palaeontological data – charophytes, palynomorphs, ostracods– are provided. Ariño arguably represents the most prolific and palaeobiologically diverse locality in which fossiliferous amber and a dinosaur bonebed have been found in association, and the only one known where the vast majority of the palaeontological assemblage suffered no or low-grade pre-burial transport. That has enabled unlocking unprecedentedly complete and reliable palaeoecological data out of two complementary windows of preservation from the same site.

Introduction

Localities preserving either vertebrate bonebeds or fossilised plant resin (amber) are among the most valuable sources of information on past terrestrial ecosystems (***Rogers et al., 2007; Seyfullah et al., 2018***). Yet, when a bonebed and fossilised resin are found jointly in the same site, and there is certainty that they originally belonged to the same biocoenosis, the potential for extracting and integrating palaeobiological data is barely unmatched in palaeontology. Although amber from the Cretaceous is often found together with other fossils such as plant and, more infrequently, vertebrate remains, fossiliferous amber associated with bonebeds including dinosaurs has been previously reported in only three occasions. Firstly, the lower Cenomanian (ca. 96–100.5 Ma) locality of Fouras/Bois Vert (Charente-Maritime, France) yielded diverse vertebrate remains –including about 50 dinosaur

bone fragments–, plant macroremains, molluscs, and amber lumps, a few of which were fossiliferous (***Néraudeau et al., 2003***). From the latter, ~110 bioinclusions belonging to arachnids, springtails and, at least, four insect orders have been reported, including several species described (***Perrichot et al., 2007; Tihelka et al., 2021***). Secondly, amber is known from the upper Campanian (~73 Ma) Pipestone Creek bonebed (Alberta, Canada) (***Tanke, 2004; Currie et al., 2008***). Although >99% of the 3,000 individual fossils recovered from this site belong to *Pachyrhinosaurus*, other dinosaurs, fish, turtles, lizards, and crocodilians were found (***Bell and Currie, 2006; Currie et al., 2008; Cockx et al., 2020***). Six bioinclusions recovered from ca. 50 cm^3 of typically <1 cm amber pieces were described (***Cockx et al., 2020***). Lastly, fossiliferous amber was found in the Stratum 11 from the uppermost Maastrichtian (ca. 67–66 Ma) Bone Butte bonebed site (South Dakota, USA) (***DePalma, 2010***). This site, belonging to the intensively-studied Hell Creek Formation (Fm.), provided ~3,000 mostly disarticulated fossils representing >50 species of dinosaurs and other vertebrates; the non-vertebrate material included molluscs, ichnofossils, and plant macroremains, and was mostly found together with the fossiliferous amber (***DePalma, 2010; DePalma et al., 2015***). The palaeodiversity recovered from the latter, in contrast, was rather scarce, with 22 bioinclusions found in 400 g of collected amber (***DePalma, 2010; DePalma et al., 2010; Nel et al., 2010***). Other Bone Butte strata yielded non-fossiliferous amber (***DePalma, 2010***). In addition, a hadrosaur jaw with an amber piece originally attached to it and containing an inclusion was reported from the uppermost Campanian Dinosaur Park Fm. in Alberta (***McKellar et al., 2019***). Further Upper Cretaceous bonebed localities from western Canada yielded amber but lacking bioinclusions (***Cockx et al., 2021***).

The Ariño deposit represents one of the most important Lower Cretaceous dinosaur sites from Europe (***Alcalá et al., 2012***). This outcrop, located within the Santa María open-pit coal mine (Ariño municipality, Teruel Province, Spain), takes part in the Oliete Sub-basin from the Maestrazgo Basin (eastern Iberian Peninsula) (***Salas and Guimerà, 1996***). This extensional sub-basin was infilled with sediments deposited in palaeoenvironments ranging from marine to continental during the early Barremian to middle Albian (***Meléndez et al., 2000***). In this sub-basin, the siliciclastic Escucha Fm., early Albian in age (***Peyrot et al., 2007; Bover-Arnal et al., 2016***), was deposited overlying Aptian marine carbonates (***Cervera et al., 1976***). This formation represents coastal environments that included barrier-island systems with back-barrier marshes and flood-tidal deltas (***Rodríguez-López et al., 2009***). The AR-1 level of the Ariño locality, with ca. 600,000 m^2 of surveyed surface, consists of marls with a high concentration of organic matter occasionally forming coal which underlie the lowest level of coal exploited in the Santa María mine (***Figure 1, Supplementary Video 1***) (***Alcalá et al., 2012***). The AR-1 level has yielded a rich and diverse vertebrate fossil record representing more than 10,000 fossils namely found in more than 160 mono- or bitaxic concentrations of usually well-preserved, articulated or semi-articulated partial skeletons (***Alcalá et al., 2012, 2018; Buscalioni et al., 2013; Villanueva-Amadoz et al., 2015***). From these, new species of freshwater and terrestrial turtles, crocodilians, and ornithischian dinosaurs –i.e., the ornithopod *Proa valdearinnoensis* and the nodosaurid *Europelta carbonensis*– have been described (***McDonald et al., 2012; Buscalioni et al., 2013; Kirkland et al., 2013; Pérez-García et al., 2015, 2020***). Predatory dinosaurs were also present in the Ariño ecosystem, as evidenced by coprolites, ichnites, and isolated allosauroidean teeth (***Alcalá et al., 2012, 2018; Vajda et al., 2016***). Chondrichthyan

and osteichthyan fish remains have also been occasionally found (***Alcalá et al., 2012***). Regarding the invertebrate record, three ostracod species (***Tibert et al., 2013***), as well as freshwater bivalves and gastropods, were reported (***Alcalá et al., 2012; Kirkland et al., 2013***). From the palaeobotanical standpoint, two charophyte species, fern remains, conifer twigs, taxonomically unassigned charcoalified wood remains, undetermined cuticles, and palynomorphs found in both the marls and coprolites (spores, gymnosperm, and angiosperm pollen grains) were previously known (***Tibert et al., 2013; Villanueva-Amadoz et al., 2015; Vajda et al., 2016***). Based on the former geological and palaeontological data, the Ariño palaeoenvironment was inferred as a freshwater swamp plain with perennial alkaline shallow lakes subjected to salinity fluctuations due to marine influence under a tropical–subtropical climate (***Alcalá et al., 2012; Tibert et al., 2013; Villanueva-Amadoz et al., 2015***). The level AR-1 was dated as early Albian (ca. 110 Ma) based on charophyte, palynological, and ostracod assemblages (***Tibert et al., 2013; Villanueva-Amadoz et al., 2015; Vajda et al., 2016***).

The presence of indeterminate amounts of amber in the AR-1 level from Ariño was first noted by ***Alcalá et al. (2012)***, with later works only adding that amber pieces were abundant and sometimes large (***Alcalá et al., 2018***). The only hitherto described bioinclusion from Ariño amber was a tuft of three remarkably well-preserved mammalian hair strands corresponding to the oldest hair reported in amber (***Álvarez-Parra et al., 2020a).***

In the Iberian Peninsula, amber is found in Triassic (Ladinian–Rhaetian) and Cretaceous (Albian–Maastrichtian) deposits; those having yielded abundant amber with bioinclusions are mostly late Albian in age, namely from the Basque-Cantabrian (e.g., Peñacerrada I and El Soplao) and Maestrazgo basins (e.g., San Just) (***Alonso***

149 ***et al., 2000; Delclòs et al., 2007; Peñalver et al., 2007; Najarro et al., 2009;***
150 ***Peñalver and Delclòs, 2010***).

151 Here, we characterise the amber deposit associated with the dinosaur bonebed
152 AR-1 of Ariño from a multidisciplinary standpoint, describing its morphological,
153 geochemical, palaeofaunistic, and taphonomic features, all of which allow to
154 recognise the palaeobiological singularity of the site. Together with complementary
155 palaeontological data (charophytes, palynomorphs, ostracods), our results enable a
156 complete palaeoecological reconstruction of this unique locality.

157

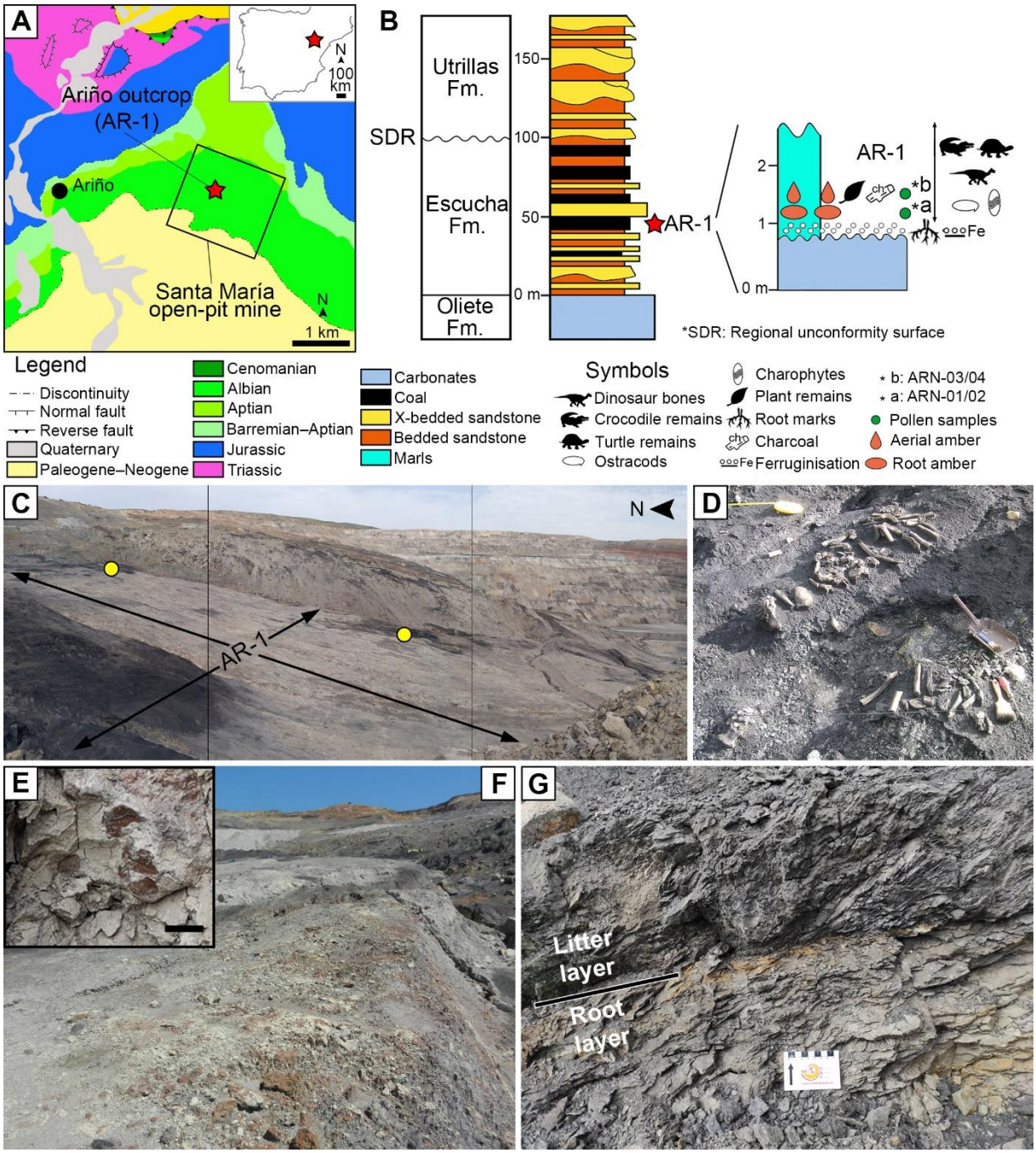

Figure 1. The Lower Cretaceous vertebrate bonebed and amber site of Ariño. (**A**) Geographical and geological location; modified from ***Alcalá et al. (2012)*** (**B**) Stratigraphic location of the level AR-1; general stratigraphic log from the Oliete Sub-basin, modified from ***Kirkland et al. (2013)***, is shown at the left, together with the location of the level AR-1 (red star); a section of the latter, including the stratigraphic location of the amber deposit studied herein, is shown at the right. (**C**) Santa María open-pit coal mine with indication of the level AR-1 and the two excavated areas rich

in aerial amber (yellow dots); the bottom of the open-pit coal is at the right. (**D**) One of the 160+ bone concentrations found in Ariño, AR-1/10, during vertebrate fieldwork in 2010, showing the holotype of the nodosaurid *Europelta carbonensis*; metal dustpan ~30 cm long. (**E**) Root marks at the top of the carbonates below the level AR-1; scale bar, 1 cm. (**F**) Carbonates right below the level AR-1, displaying edaphic features at the top. (**G**) Detail photograph of the level AR-1 showing the lower root layer (with amber from resin exuded by roots) and the upper litter layer (with amber from resin exuded by trunk and branches); centimetric scale. See also ***Supplementary Video 1***.

Results

Amber characteristics

Two distinct amber-bearing layers, a lower one and an upper one, are present in the Ariño AR-1 level (***Figures 1, 2—figure supplements 1 and 2***). The lower layer overlies a level of carbonates of oligotrophic lacustrine origin showing the development of palaeosols at its top, including root marks (***Figure 1E,F***). This layer is characterised by abundant, irregular amber lumps (i.e., kidney-shaped) 10–40 cm in length with protrusions, an opaque crust, an inner banding pattern, and lacking bioinclusions (***Figure 2A,C,F—figure supplement 1***). Aerial amber and charcoalified plant remains are absent in this layer. The kidney-shaped amber pieces are distributed along the exposed area of the AR-1 level and, if not partially exposed due to weathering, are complete. The opaque crust from the amber pieces has an irregular morphology and its ultrastructure shows delicate microprotrusions and no evidence of linear grooves (***Figure 2C–E***). The banding patterns are formed by

191 variable densities of abundant bubble-like inclusions of different sizes and which are
192 monophasic (solid), biphasic (solid + liquid), or triphasic (solid + liquid + gas) (***Figure***
193 ***2G***). Mineral crystals have been detected growing inwards inside allegedly empty
194 spaces left by larger bubble-like inclusions – these include pyrite cuboctahedrons
195 and needle-shaped crystals from an iron sulphate mineral according to EDS analysis
196 (likely szomolnokite, $Fe^{2+}SO_4 \cdot H_2O$) (***Figure 2H,I—figure supplement 3A***).
197 The upper layer from the Ariño AR-1 level is rich in amber pieces of flow-,
198 droplet-, and stalactite-shaped morphologies, and often showing external and/or
199 internal desiccation surfaces (***Figure 2B—figure supplement 2***). Small, almost
200 spherical amber pieces about 1–5 cm in diameter, with an opaque crust similar to the
201 kidney-shaped amber pieces, are also present in this layer, yet scarcely; their surface
202 is polished and more regular in patterning (***Figure 2—figure supplement 3B–D***).
203 Amber pieces range from translucent to opaque, and from light yellow to dark reddish
204 in colour. One peculiar piece showed subtle, multidirectional surface microscopic
205 scratches and borings, the latter filled with an undetermined material, neither calcium
206 carbonate nor gypsum (***Figure 2—figure supplement 3E***).
207

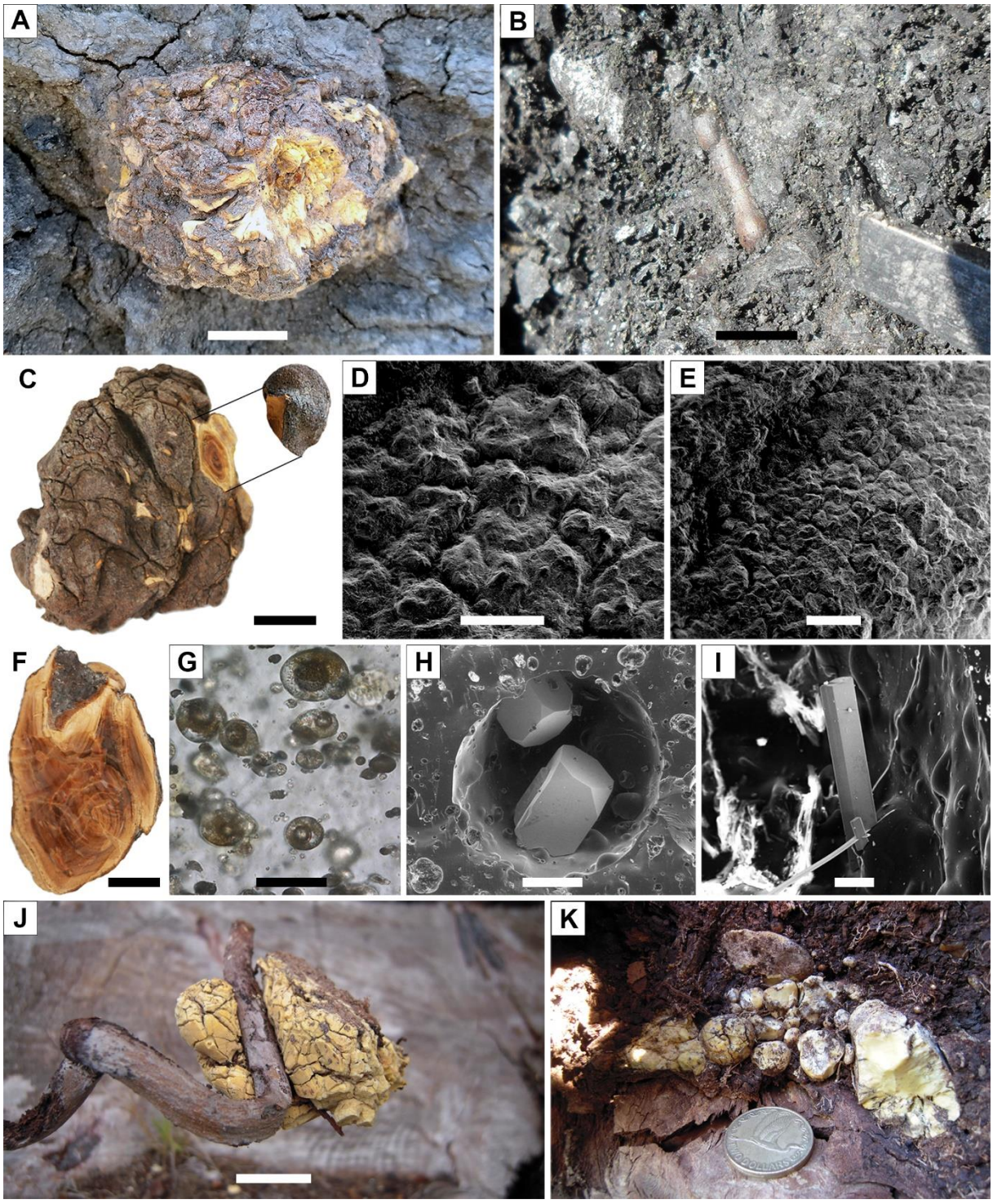

Figure 2. Diversity of amber pieces from the AR-1 level and Pleistocene copal pieces for comparison. (**A**) Kidney-shaped amber piece (root layer). (**B**) Aerial amber piece (litter layer), corresponding to a resin flow, after partially removing surrounding rock during fieldwork. (**C**) Kidney-shaped amber piece (AR-1-A-2019.93) from the root layer. (**D**, **E**) Two different areas of the external surface from a fragment detached

from the piece in (C), showing the preserved delicate surface microprotrusions and no evidence of linear grooves. (**F**) Kidney-shaped amber piece (root layer) showing the internal banding pattern (AR-1-A-2019.132). (**G**) Triphasic (solid + liquid + gas) bubble-like inclusions in a kidney-shaped amber piece (AR-1-A-2019.130). (**H**) Two pyrite cuboctahedrons in an alleged empty space left by a fluid bubble-like inclusion (amber piece AR-1-A-2019.86). (**I**) Needle-shaped crystals from an iron sulphate (likely szomolnokite) growing inward from the walls in an alleged empty space left by a fluid bubble-like inclusion (amber piece AR-1-A-2019.129). (**J**) Kidney-shaped piece of Pleistocene copal associated to an *Agathis australis* root from an overturned stump in Waipapakauri (North Island, New Zealand). (**K**) Pleistocene copal pieces associated to the root system of the same *A. australis* stump; coin 2.65 cm in diameter. Scale bars, 2 cm (A–C, F, J), 0.5 mm (D), 1 mm (E), 0.03 mm (G), 0.2 mm (H), and 0.1 mm (I). See also ***Supplementary Video 1***.

The FTIR spectra of two stalactite-shaped amber pieces from Ariño are dominated by a small C-H stretching band at 2925 cm^{-1}, an intense C-H band at 1457 cm^{-1}, and an intense carbonyl band at 1707 cm^{-1} (***Figure 3A*—source *data 1–3***), all characteristic of amber (***Grimalt et al., 1988***). Hydroxyl bands near 3500 cm^{-1} are present. The Ariño amber spectra are very similar to those from San Just amber, their main difference being the presence of a small band near 1200 cm-1 in the latter. On the other hand, the composition of the organic solvent-extractable materials obtained by GC-MS, comprising the 32.5% of the Ariño amber, is dominated by labdane resin acids and its diagenetic derivatives, with amberene (**I**; 1,6-dimethyl-5-isopentyltetralin) being the major component in the bulk extract (***Figure 3B*—*figure supplement 1*—*source data 4***). The labdan-18-oic acids are dominant in the polar

239 fraction of the organic extract from the amber. The identification of the clerodane-
240 family diterpene **VI** is noteworthy. The analyses show no evidence of significant
241 terpenes of the pimarane/abietane family and discard the presence of ferruginol. The
242 Ariño amber does not show a significant content of neither 15-homoamberene (**III**)
243 nor 1-methylamberene (**X**) (***Figure 3B—figure supplement 1***) (***Kawamura et al.,***
244 ***2018***). This could point to a lack of the corresponding labdanoid alcohols or non-
245 oxidised C18/C19 labdanoids in the precursor resin, as the diagenesis of these
246 molecules could lead to 1-methylamberene. The decarboxylation of the labdan-18-oic
247 acids prevailing in the Ariño amber polar fraction could be the first step in the
248 diagenesis to amberene and its related compounds, especially isomers of the
249 labdanoid **VI**, found as a rich distribution of peaks with M^+=246.
250

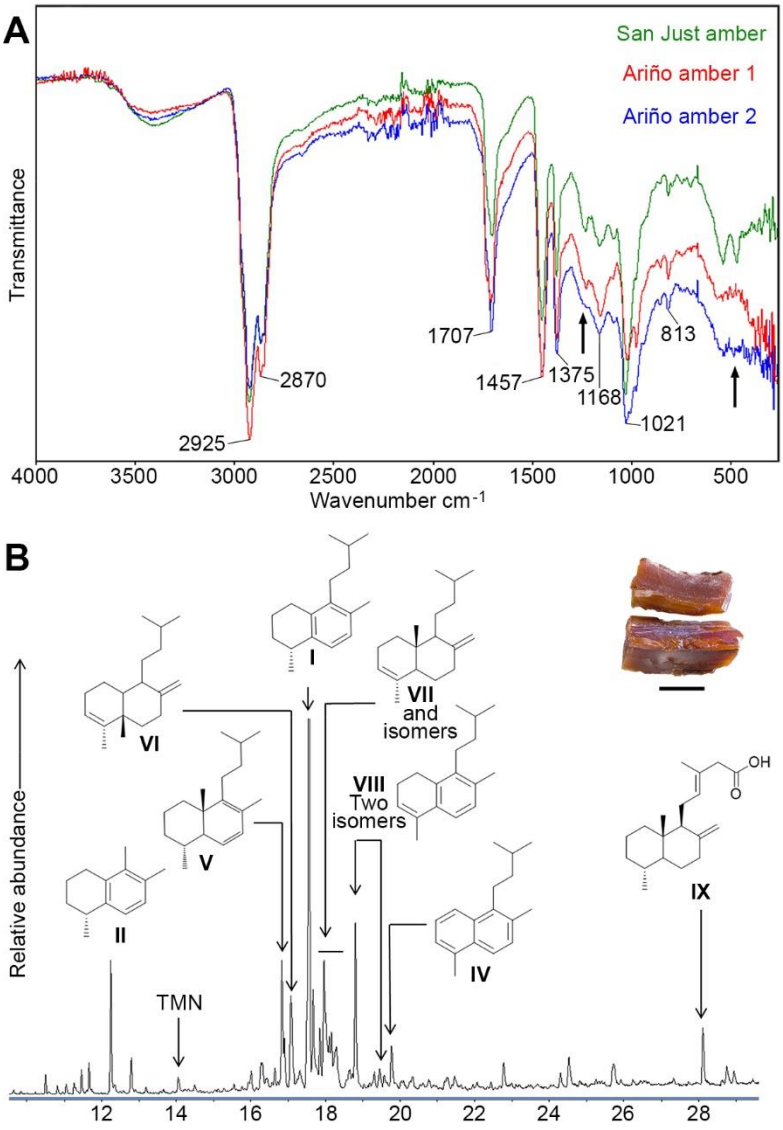

Figure 3. Physicochemical characterisation of the Lower Cretaceous amber from Ariño. (**A**) Infrared (FTIR) spectra obtained from two aerial amber pieces (litter layer); a spectrum from San Just amber (upper Albian) is provided for comparison; arrows indicate the main differences between Ariño and San Just ambers, at around 1200 and 500 cm^{-1}; resolution = 4 cm^{-1}. (**B**) Gas chromatography-mass spectrometry (GC-MS) trace for the underivatised total solvent extract of aerial amber, showing the structures of the main identified terpenoids, referred herein using Roman numerals (full formulation provided in ***Figure 3—figure supplement 1B***); TMN =

trimethylnaphthalenes; the analysed aerial amber is shown at the top right (scale bar 0.5 mm).

Bioinclusions

A total of 166 bioinclusions were obtained out of 918 g of aerial amber (***Figure 4—figure supplement 1***); about one third of them are well to exceptionally well preserved. Plant inclusions are present, such as numerous fern or conifer trichomes (not considered in the inclusion recount) and other undetermined remains (***Figure 4—figure supplement 1A–E***). The diverse assemblage is namely composed of arthropods or remains of their activity, such as spiderweb threads (***Figure 4—figure supplement 1F,G***) and coprolites, but also a few vertebrate integumentary remains. Arthropods are represented by arachnids and 11 insect orders. Arachnid inclusions belong to mites (Acari) and spiders (Araneae). Mites include a rare trombidiform of the family Rhagidiidae, an oribatid, and an undetermined six-legged larva (***Figure 4A***). One spider offers taphonomic insights (***Figure 4—figure supplement 1H***). Five amber pieces with arthropods as syninclusions have spiderwebs preserved; although all are isolated strands, one tangled sample might correspond to a partial web (***Figure 4—figure supplement 1F***). In the latter, glue droplets on several strands suggest it belonged to an orb web (***Figure 4—figure supplement 1G***). The insect orders found in the Ariño amber are jumping bristletails (Archaeognatha), crickets (Orthoptera), cockroaches (Blattodea), barklice (Psocodea), thrips (Thysanoptera), whiteflies and aphids (Hemiptera), lacewings (Neuroptera), beetles (Coleoptera), moths (Lepidoptera), gnats, midges, and other flies (Diptera), and wasps (Hymenoptera). Archaeognaths are represented by the inclusion of a cercus and a medial caudal filament. Two orthopterans are poorly preserved, but one could belong

285 to †Elcanidae. A blattodean nymph and an adult have been found, as well as several
286 remains such as probably blattodean isolated antennae. Among the seven
287 psocodeans discovered, new taxa probably within the †Archaeatropidae and
288 Manicapsocidae have been recognised. Thysanopterans are the third most abundant
289 insect order in the Ariño amber, with 11 specimens (***Figure 4B,C***); three amber
290 pieces contain more than one thrips as syninclusions. One isolated thrips shows a
291 thin milky coating (***Figure 4—figure supplement 1I***), also found in other inclusions,
292 and an infrequent nymph is unusually well preserved (***Figure 4B***). Hemipterans
293 comprise four representatives of Sternorrhyncha and two incomplete undetermined
294 specimens. Three of the former have been identified as Aleyrodidae, probably
295 belonging to the Aleurodicinae (***Figure 4D***), and are preserved in the same amber
296 piece as syninclusions. In addition, an Aphidoidea is found in an amber piece with
297 spiderweb strands. The neuropteran record consists of two wing impressions on
298 amber surfaces probably belonging to Berothidae and a complete specimen, which
299 could correspond to a †Paradoxosisyrinae (Sisyridae). Five coleopteran specimens
300 have been discovered, two tentatively identified as belonging to Cantharidae and
301 Ptinidae. A ditrysian lepidopteran larva, yet incomplete anteriorly, is remarkably well
302 preserved (***Figure 4E***). Dipterans (***Figure 4F***) are represented by 19 specimens of
303 the families †Archizelmiridae, Cecidomyiidae, Ceratopogonidae (including at least
304 one female), Chironomidae, Mycetophilidae, Rhagionidae, Scatopsidae, and
305 probably Psychodidae. The first group is represented by a well-preserved male within
306 the genus *Burmazelmira* (***Figure 4F***). Lastly, hymenopterans are the most abundant
307 insects in Ariño amber, accounting for 34 specimens belonging to the
308 Platygastroidea, Mymarommatoidea, †Serphitidae, and †Stigmaphronidae (***Figure***

309 ***4G–I***). Furthermore, a new vertebrate inclusion is represented by a basal feather

310 portion of pennaceous structure (***Figure 4J***).

311

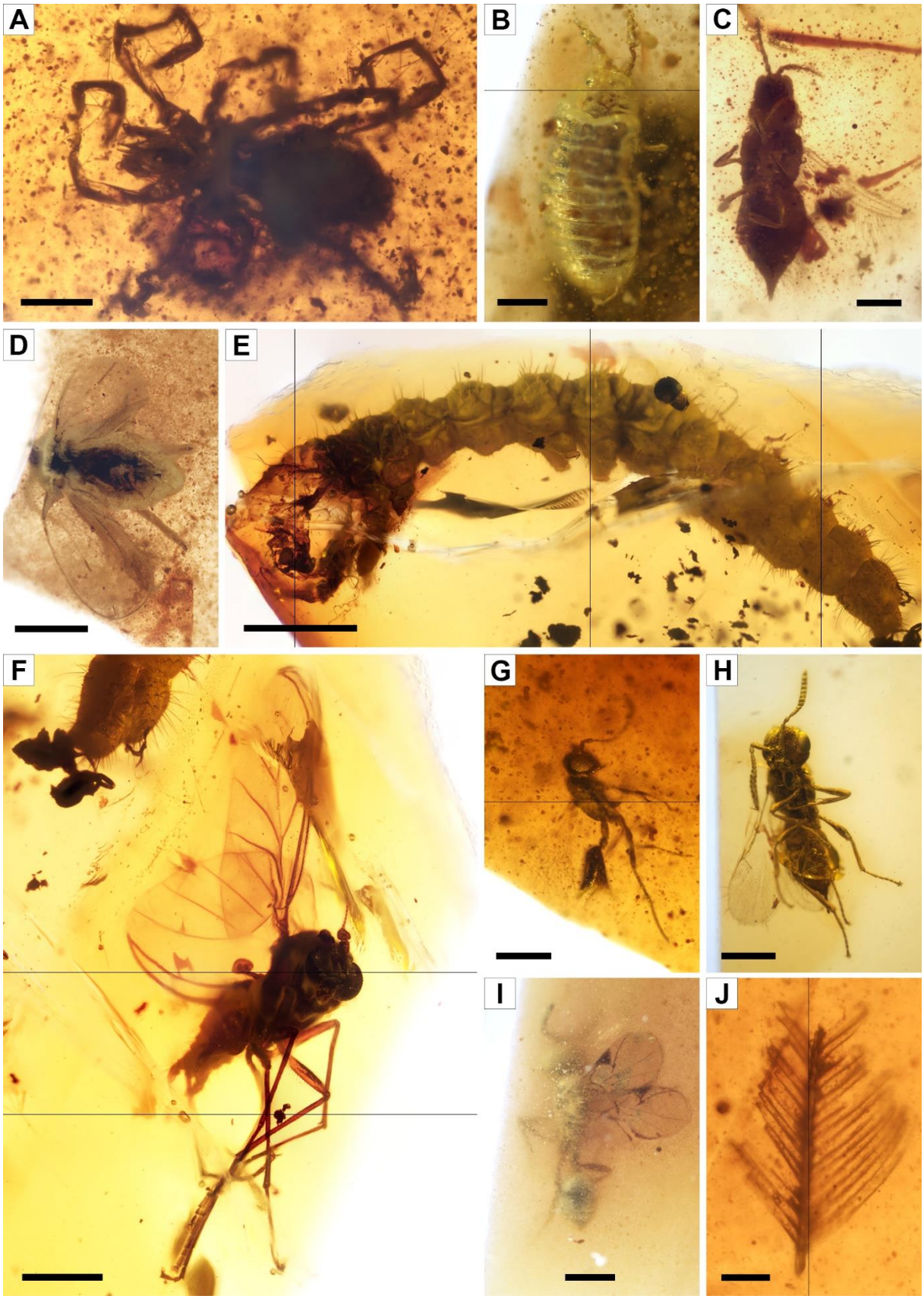

Figure 4. Faunal bioinclusions from the Lower Cretaceous bonebed amber of Ariño. (**A**) A rhagidiid mite, the oldest known (Acari: Rhagidiidae; AR-1-A-2019.71). (**B**) An

315 immature thrips (Thysanoptera; AR-1-A-2019.114.2). (**C**) An adult thrips
316 (Thysanoptera; AR-1-A-2019.40). (**D**) A whitefly (Hemiptera: Aleyrodidae; AR-1-A-
317 2019.100.1). (**E**) A ditrysian lepidopteran larva (AR-1-A-2019.95.1). (**F**) A
318 *Burmazelmira* sp. fly (Diptera: †Archizelmiridae: AR-1-A-2019.95.2). (**G**) A false fairy
319 wasp, the oldest known (Hymenoptera: Mymarommatoidea; AR-1-A-2019.61). (**H**) A
320 superbly preserved platygastroid wasp (Hymenoptera: Platygastroidea; AR-1-A-
321 2019.95.3). (**I**) A serphitid wasp, the oldest known (Hymenoptera: †Serphitidae; AR-
322 1-A-2019.94.8). (**J**) A feather fragment of pennaceous structure (Theropoda; AR-1-A-
323 2019.53). Scale bars, 0.2 mm (A–C, G), 0.5 mm (D, F, H, I), 1 mm (E), and 0.1 mm
324 (J).
325
326 **Palaeobotanical and ostracod assemblages**
327 Charophytes sampled from the level AR-1 comprise four species belonging to the
328 families †Clavatoraceae and Characeae. The assemblage is dominated by
329 †Clavatoraceae, namely by well-preserved fructifications of *Atopochara trivolvis* var.
330 *trivolvis* (***Figure 5A–D—figure supplement 1A,B***) and *Clavator harrisii* var. *harrisii*
331 (***Figure 5E–J—figure supplement 1C–E***) (n>100 for each species). The former is
332 represented by large utricles showing a characteristic triradiate symmetry and
333 displaying flame-shaped cells at positions a1, a3, b1 and c1 (***Grambast, 1968***); such
334 configuration is variable in other populations of the same species. Five morphotypes
335 of *C. harrisii* var. *harrisii* have been distinguished based on the cell disposition at the
336 abaxial side of the utricle, showing the phylloid imprint flanked at the base by two
337 small cells and bearing above a complex of five to eleven cells (***Figure 5—figure***
338 ***supplement 1F–J***); although this variety had been previously identified in Ariño,
339 none of the described morphotypes were evident (***Tibert et al., 2013***), neither in

other *C. harrisii* var. *harrisii* populations worldwide. Moreover, several (n=10) portions of clavatoracean thalli belonging to *Clavatoraxis* sp. have been recovered (***Figure 5K***). Lastly, rare occurrences (n=3) of small characean gyrogonites affine to *Mesochara harrisii* are also present (***Figure 5L***); their determination remains somewhat uncertain due to the lack of basal plate (***Martín-Closas et al., 2018***).

Charcoalified plant remains (fusinite/inertinite) are abundant in the upper amber layer (***Figure 2—figure supplement 2A***). These correspond to secondary xylem with strongly araucariacean (1) 2 (3) seriate intertracheary radial pitting and araucarioid cross-fields. Although they are similar to the araucariacean *Agathoxylon gardoniense*, we prefer to identify these samples as *Agathoxylon* sp. due to preservation. Other charcoalified wood remains likely belonging to other taxonomic groups have also been found. Furthermore, a rare sample of amber-filled plant tissue shows cells elliptic to rounded in cross-section and elongate in longitudinal section, blunt tips, 20–50 µm in diameter, and with thin walls (somewhat collenchymatous). Cells are arranged radially, but without evidence of growth rings. These characteristics suggest that this fossilised tissue might represent suber (cork) (***Figure 4—figure supplement 1B–E***).

The four studied palynological samples (ARN-01–ARN-04) have provided highly diverse, well-preserved assemblages that include a total of 72 different palynomorph taxa, i.e., two from freshwater algae, 38 from spores of ferns and allied groups, 21 from gymnosperm pollen grains, and 11 from angiosperm pollen grains (***Figure 5M–T—figure supplement 1K–P, Supplementary Table 1***). Aquatic palynomorphs, consisting of zygnematacean freshwater algae, are a small proportion of the samples except for ARN-04, characterised by the abundance of *Chomotriletes minor* (3.87% of the total palynomorph sum) (***Figure 5M***). Spores numerically dominate the

assemblages except for ARN-01. Overall, fern spores (13.48–38.42%), such as *Appendicisporites* spp. (***Figure 5N***), *Cicatricosisporites* spp., *Cyathidites australis*, *Cyathidites minor* (***Figure 5O***), and *Gleicheniidites senonicus*, predominate over those of bryophytes and lycophytes (1.44–2.38%). Gymnosperms are namely represented by *Inaperturopollenites dubius* (12.79–20.36%) (***Figure 5P***), related to taxodioid conifers (***Stuchlik et al., 2002***), and the genus *Classopollis* (9.39–15.95%) (***Figure 5Q***), produced by †Cheirolepidiaceae conifers (***Taylor and Alvin, 1984***). Araucariacean and bisaccate pollen show low amounts except for the araucariacean *Araucariacites* spp. (***Figure 5R***), which is particularly abundant in ARN-01 (12.79%). The abundance of *Eucommiidites* spp., assigned to †Erdtmanithecaceae gymnosperms, is also relevant (2.90–8.00%) (***Figure 5S***). "*Liliacidites*" *minutus* (***Figure 5T***) was the most abundant angiosperm pollen in the assemblages (up to 12% in ARN-01).

The ostracod fauna recovered from the level AR-1 is comprised of four species belonging to the families Limnocytheridae, †Cyprideidae, and Cyprididae (***Figure 5U–EE—figure supplement 1Q–Y***). Specimens show mostly closed carapaces and are generally well preserved. The Limnocytheridae are represented by *Theriosynoecum* cf. *fittoni* (***Figure 5U,V***) (n=20) and *Rosacythere denticulata* (n>70) (***Figure 5W–BB***). Although the latter species was previously identified in Ariño (***Tibert et al., 2013***), three variants have now been detected: one with a faint pitting and extremely small rosette ornamentation (***Figure 5W***), one with a well-developed rosette (***Figure 5X,Y,AA—figure supplement 1Q–U***), and one with strongly developed rosette and spine-like nodes locally generated at the postero-dorsal and postero-ventral parts of the carapace (***Figure 5Z,BB—figure supplement 1V–Y).*** †Cyprideidae and Cyprididae are found for the first time in Ariño, represented by the

390 species *Cypridea* cf. *clavata* (n=35) (***Figure 5CC,DD***) and *Mantelliana* sp. (n=12)

391 (***Figure 5EE***), respectively.

392

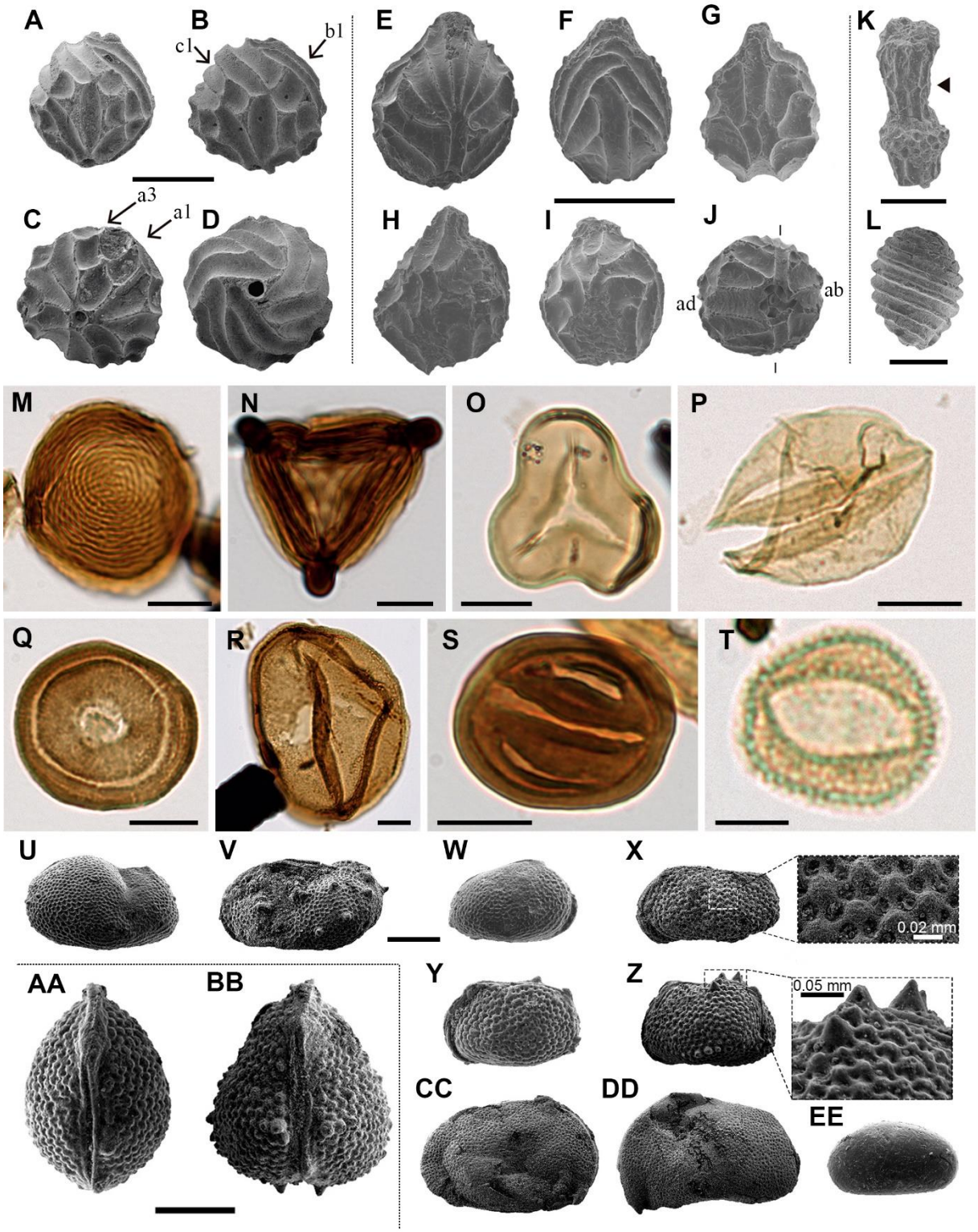

393

Figure 5. Charophyte (A–L), palynomorph (M–T), and ostracod (U–EE) records sampled from level AR-1 of Ariño. (**A**–**D**) *Atopochara trivolvis* var. *trivolvis* (†Clavatoraceae): (**A**, **B**) Lateral views (AR-1-CH-004 and AR-1-CH-005, respectively); (**C**) Basal view (AR-1-CH-007); (**D**) Apical view (AR-1-CH-008); cell lettering after ***Grambast (1968)***. (**E**–**J**) *Clavator harrisii* var. *harrisii* (†Clavatoraceae): (**E**) Lateral view (AR-1-CH-009); (**F**) Adaxial view (AR-1-CH-011); (**G**) Abaxial view morphotype II (AR-1-CH-013); (**H**) Abaxial view morphotype III (AR-1-CH-014); (**I**) Abaxial view morphotype IV (AR-1-CH-015); (**J**) Basal view (AR-1-CH-017) with indication of adaxial (ad) and abaxial (ab) sides. (**K**) *Clavatoraxis* sp. (†Clavatoraceae) (AR-1-CH-019); the arrowhead indicates the zig-zag line at the central part of the internode. (**L**) aff. *Mesochara harrisii* (Characeae) in lateral view (AR-1-CH-001). (**M**) *Chomotriletes minor* (ARN-03). (**N**) *Appendicisporites tricornitatus* (ARN-01). (**O**) *Cyathidites minor* (ARN-02). (**P**) *Inaperturopollenites dubius* (ARN-04). (**Q**) *Classopollis* sp. (ARN-02). (**R**) *Araucariacites hungaricus* (ARN-01). (**S**) *Eucommiidites minor* (ARN-01). (**T**) "*Liliacidites*" *minutus* (ARN-01). (**U**, **V**) *Theriosynoecum* cf. *fittoni* (Limnocytheridae): (**U**) Right lateral view, female carapace (AR-1-OS-001); (**V**) Left lateral view, male carapace (AR-1-OS-002). (**W**–**BB**) *Rosacythere denticulata* (Limnocytheridae): (**W**) Female? carapace, right lateral view, variant with extremely small rosette ornamentation (simply reticulated form) (AR-1-OS-006); (**X**) Male carapace of the variant with well-developed rosette ornamentation, left lateral view (AR-1-OS-011), and detail of the ornamentation; (**Y**) Female carapace of the variant with well-developed rosette ornamentation, left lateral view (AR-1-OS-007); (**Z**) Female carapace of the variant with strongly developed rosette ornamentation and spine-like nodes, left lateral view (AR-1-OS-015), and detail of the spine-like node ornamentation; (**AA**) Female carapace of the variant with

well-developed rosette ornamentation, dorsal view (AR-1-OS-012); (**BB**) Female carapace of the variant with strongly developed rosette ornamentation and spine-like nodes, dorsal view (AR-1-OS-018), showing intraspecific variability. (**CC**, **DD**) *Cypridea* cf. *clavata* (†Cyprideidae): (**CC**) Specimen in right lateral view (AR-1-OS-004); (**DD**) Specimen in left lateral view (AR-1-OS-005). (**EE**) *Mantelliana* sp. (Cyprididae) (AR-1-OS-003), right lateral view. Scale bars, 0.5 mm (A–J), 0.25 mm, (K) 0.2 mm (L, U–EE), 0.01 mm (M–S), and 0.005 mm (T). See also ***Supplementary Table 1***.

Discussion

The kidney-shaped, bioinclusion-lacking amber pieces from AR-1's lower amber-bearing layer were produced by roots. Subterranean accumulations from both Recent/subfossil resin in modern forests and amber in geological deposits have been partly attributed to roots (***Langenheim, 1967, 2003; Henwood, 1993; Martínez-Delclòs et al., 2004; Seyfullah et al., 2018***). Although the resiniferous capacity of roots is well known (***Langeinheim, 2003***), observations of resin attached and/or associated with roots from both angiosperms and gymnosperms have been occasional (***Langenheim, 1967; Seyfullah et al., 2018***). Our field observations of late Pleistocene copal pieces produced and still attached to roots, covered by original soil, in an *Agathis australis* overturned stump, formerly referred to but not figured (***Najarro et al., 2009; Speranza et al., 2015***), show similar morphologies to the Ariño kidney-shaped amber pieces (***Figure 2J,K***). The Ariño's lower amber layer is interpreted as a root layer where the abundant and complete amber pieces are strictly in situ, i.e., they are located exactly where the roots of the resiniferous trees

444 exuded this resin in the subsoil (***Figure 6A***). This level immediately overlies
445 carbonates that display edaphic features at the top (***Figure 1E,F***). It has high lateral
446 continuity and lacks aerial amber or charcoalified plant remains (***Figures 1, 2A—***
447 ***figure supplement 1***). Also, the fragile surface protrusions and microprotrusions of
448 the kidney-shaped amber pieces from this layer would not have preserved even if
449 minimal biostratinomic transport or other processes entailing abrasion had occurred
450 (***Figure 2C–E***). This is the first time strictly in situ amber is reported; the scarcely-
451 fossiliferous, autochthonous-parautochthonous Triassic amber droplets from the
452 Dolomites are preserved in a palaeosol (***Schmidt et al., 2012; Seyfullah et al.,***
453 ***2018***), but they are strictly ex situ, as the resin at least felt by gravity from their
454 above-ground exudation location to the forest floor (***Figure 6A***). Although other
455 amber-bearing outcrops from the Iberian Peninsula have commonly yielded kidney-
456 shaped amber pieces (***Alonso et al., 2000; Peñalver et al., 2007; Najarro et al.,***
457 ***2009***), these appear fragmented and in pockets together with aerial amber and
458 generally have smoother surfaces and more regular morphologies than those from
459 Ariño. The kidney-shaped amber pieces have further noteworthy characteristics.
460 Firstly, the amber pieces show marked internal bands composed of variable densities
461 of mono-, bi-, or triphasic bubble-like inclusions (***Figure 2F,G***). Although these
462 microscopic inclusions likely correspond to fossilissed sap-resin emulsions (***Lozano***
463 ***et al., 2020***), at least partially, they show more complex and previously
464 undocumented morphologies and arrangements. These microinclusions have the
465 potential to provide key data on taphonomy and the conditions under which resin
466 production occurred. Moreover, pyrite cuboctahedrons (***Figure 2H***) are usually found
467 as mineralisations in the alleged empty spaces left by fluid bubble-like inclusions
468 within amber (***Alonso et al., 2000***); they have been related to early diagenesis in

reducing environments produced by anaerobic bacteria (***Allison, 1990***). In contrast, the iron sulphate minerals growing in these spaces (***Figure 2I—figure supplement 3A***) have not been previously reported; they could have formed during late diagenesis under oxidising conditions after the input of oxygenised water into the amber (***Allison, 1990***). Secondly, the kidney-shaped amber pieces from Ariño lack the coating of resinicolous fungal mycelia otherwise common in Cretaceous ambers (***Speranza et al., 2015***). Both the mono- to multiphasic inclusions and the lack of fungal coating might be related to the likely partial flooding of the Ariño forest soil, typical of swampy environments. Although resin can solidify on or within the forest soil in tropical or subtropical climate environments (***Henwood, 1993***), plant macrofossils are usually highly altered and poorly preserved in soils and coal deposits (***Delclòs et al., 2020***). The absence of roots associated with the kidney-shaped amber pieces in the root layer could be explained by their differential fossilisation in the partly flooded soil.

The upper amber-bearing layer from Ariño's AR-1 level is rich in aerial amber pieces (***Figure 2B—figure supplement 2***). This amber type results from fluid resin falling on the ground from the trunk or branches along the gravity gradient (***Martínez-Delclòs et al., 2004***). The aerial amber pieces commonly have delicate morphologies and preserve external desiccation surfaces, both elements indicating very limited transport. Overall, the upper layer is interpreted as a litter layer namely resulting from the autochthonous-parautochthonous accumulation of strictly ex situ aerial amber pieces, but also occasionally containing amber pieces showing surface polishing or scratching and thus likely being more allochthonous in nature, i.e., transported and deposited far away from its production environment (***Figure 6A***). Moreover, the absence of strictly in situ kidney-shaped amber pieces in the litter layer

494 suggests that AR-1 corresponds to a single cycle of forest floor installation-
495 destruction. On the contrary, charcoalified wood remains are abundant in this layer;
496 these were previously found in Ariño and were related to wildfires (***Villanueva-***
497 ***Amadoz et al., 2015; Vajda et al., 2016***), which have been deemed as promoters of
498 resin production and accumulation (***Najarro et al., 2010; Seyfullah et al., 2018***). On
499 the other hand, the aerial amber is highly fossiliferous, with 145 bioinclusions/kg
500 (excluding coprolites, spiderwebs, and undetermined bioinclusions). Although
501 determining amber bioinclusion richness is prone to multiple biases (e.g., bioinclusion
502 recounting should be ideally limited to aerial amber, as kidney-shaped amber
503 fragments were almost certainly devoid of bioinclusions), this value is among the
504 highest reported worldwide. Richness data from other Cretaceous Albian to
505 Cenomanian amber localities range from about 10 to 80 inclusions/kg (***Grimaldi et***
506 ***al., 2002; Néraudeau et al., 2002; Girard et al., 2013; Peñalver et al., 2018; Zheng***
507 ***et al., 2018***), although values surpassing the 500 insects/kg have been exceptionally
508 reported (***Rasnitsyn and Quicke, 2002***). A few bioinclusions are covered by a white
509 foam consisting of microscopic bubbles produced by decomposition fluids during
510 early diagenesis (***Figure 4—figure supplement 1I***), similar to that commonly
511 observed in the Eocene Baltic amber (***Martínez-Delclòs et al., 2004***), but otherwise
512 rare among Cretaceous ambers.

513 The charophyte, palynological, and ostracod data provided herein are also
514 indicative of a very limited transport of these remains prior to burial. The utricles of
515 the two clavatoracean charophytes found are well preserved and abundant,
516 suggesting that these remains are autochthonous. The occurrence of clavatoracean
517 portions of thalli associated with the fructifications supports this inference. The
518 studied palynological samples show conspicuous abundances of pollen related to

519 araucariacean trees and angiosperms in ARN-01 (root layer), which could indicate
520 parautochthony based on their limited pollen production and dispersal potential
521 (***Taylor and Hu, 2010***). Samples ARN-03 and ARN-04 (litter layer) contain low
522 araucariacean and angiosperm pollen and high amounts of allochthonous wind-
523 transported miospores such as *Cyathidites* spp., *Inaperturopollenites dubius*, and
524 *Classopollis* spp., which suggest chiefly allochthonous assemblages. In contrast,
525 ARN-02 (at the top of the root layer) shows a parautochthonous-allochthonous
526 transitional assemblage based on an increase of fern spores and erdtmanithecalean
527 pollen, as well as lower values of araucariacean pollen than ARN-03 and ARN-04.
528 The previous palaeobotanical accounts from Ariño concluded parautochthony based
529 on the good palynomorph preservation, some samples even showing their original
530 tetrad configuration, although they recognised that some charcoalified wood remains
531 could be allochthonous (***Villanueva-Amadoz et al., 2015; Vajda et al., 2016***). Lastly,
532 the studied ostracods constitute a relatively rich assemblage characterised by
533 abundant specimens with closed carapaces (***Figure 5AA,BB***), which together with
534 the low percentage of broken individuals points out to autochthonous remains
535 (***Trabelsi et al., 2021***).

536 The previous taphonomic accounts on the Ariño vertebrates indicated the
537 absence or lowest grade of biostratinomic transport. The abundant vertebrate fossils
538 are namely found in monotaxic (occasionally bitaxic) concentrations of well-
539 preserved, articulated, or semi-articulated remains (***Alcalá et al., 2012, 2018;***
540 ***Buscalioni et al., 2013; Villanueva-Amadoz et al., 2015***). Coprolites, likely
541 dinosaurian, show a palynomorph composition similar to that of the rock (***Vajda et***
542 ***al., 2016***). By integrating all the taphonomic data from the diverse palaeobiological
543 elements from Ariño, we can conclude that the great majority of the assemblage,

except for some pollen and charcoalified plant material, as well as a small percentage of the amber, had an autochthonous or parautochthonous origin, and therefore roughly inhabited or was produced in the same area where it fossilised. This circumstance, although critical for inferring reliable data on the palaeoecosystem (***Martínez-Delclòs et al., 2004***), remains infrequent among palaeontological deposits, particularly those jointly preserving dinosaur remains and fossiliferous amber. Indeed, the three previously reported localities where fossiliferous amber was found associated with dinosaur bonebeds, all from the Late Cretaceous, show clear signs of being either allochthonous or clearly mixed assemblages in which at least a substantial part of the vertebrate remains suffered significant transport prior to burial (***Néraudeau et al., 2003; Currie et al., 2008; DePalma, 2010***): (1) Fouras/Bois Vert (= “Plage de la Vierge”) was interpreted as resulting from a catastrophic event such as a storm in a coastal estuarine environment, with the fragmentary bones showing evidence of considerable pre-burial transport; however, amber was assumed to be not heavily transported due to the lack of rounding (***Néraudeau et al., 2003***); (2) the Pipestone Creek monodominant vertebrate assemblage corresponds to disarticulated bones formed by a fluvial allochthonous accumulation in a vegetated floodplain, and interpreted as a mass mortality event; no taphonomic assessment for the amber was provided (***Tanke, 2004; Currie et al., 2008; Cockx et al., 2020***); and (3) Bone Butte’s Stratum 11 was reconstructed as a mixed (~70/30) autochthonous/allochthonous vertebrate assemblage deposited in a river oxbow lake; amber showed no signs of significant transport (***DePalma, 2010***). From the diagenetic standpoint, a high maturity of the Ariño amber samples is inferred based on the absence of exocyclic methylenic bands at 880 cm^{-1}, 1640 cm^{-1}, and 3070 cm^{-1} in the FTIR spectra, in accordance with their Cretaceous age (***Grimalt et al., 1988***).

Furthermore, there is no significant difference in the distribution of trimethylnaphthalene isomers between the Ariño amber and the other ambarene-rich Cretaceous Iberian ambers in the GC-MS analyses (***Menor-Salván et al., 2016***), suggesting a similar thermal and diagenetic history (***Strachan et al., 1988).***

Identifying which plant sources originated the resin accumulations that led to the present amber deposits is still contentious, and different conifer groups have been proposed for the Cretaceous: †Cheirolepidiaceae, Araucariaceae, and Cupressaceae in Laurasia and other groups such as †Erdtmanithecales in Gondwana (***Menor-Salván et al., 2016; Seyfullah et al., 2020***). The GC-MS results (***Figure 3B—figure supplement 1***) classify the Ariño amber among the amberene-rich group of Cretaceous Iberian ambers. On that regard, Ariño shows the same distribution as other Iberian ambers such as those from Peñacerrada I and San Just in terpenes **I**, **II**, **V**, **VI**, and the alkylnaphthalene **IV**, resulting from the labdane aromatisation, as well as in the overall diterpene composition (***Menor-Salván et al., 2016***). This amberene-rich group is distinguished from the abietane-rich group of Cretaceous Iberian ambers (e.g., El Soplao amber) in the lack of significant terpenes from the pimarane/abietane family as well as ferruginol, a common biomarker of extant Cupressaceae (***Menor-Salván et al., 2016***). Instead, the clerodane-family diterpene **VI** found in Ariño amber, a biomarker of the family Araucariaceae (***Cox, et al., 2007***), could indicate that the botanical source of the amber is related to *Araucaria*/*Agathis*. In fact, the resin of *Araucaria bidwillii* is rich in kolavenic acid (***Cox et al., 2007***), which might be a biological precursor of **VI**. The Ariño amber differs from extant Araucariaceae in the lack of pimarane/abietane-class terpenoids. It is possible that early Araucariaceae lacked the biochemical routes of tricyclic diterpenoids that extant representatives possess (***Menor-Salván et al., 2016***). In any case, the most

plausible stance for now is to regard the Ariño amber as resulting from araucariacean resin. The finding of charcoalified *Agathoxylon* sp. supports this stance, although other types of charcoalified wood likely belonging to other taxonomic groups have been found in Ariño. The presence of araucariacean remains as bioinclusions in Albian amber from the Peñacerrada I locality was proposed as evidence for an araucariacean resin-producing tree (***Kvaček et al., 2018***). Araucariaceans have also been proposed as the source of other Lower Cretaceous ambers such as those from Lebanon, Myanmar, or France (***Poinar et al., 2007***; ***Perrichot et al., 2010***; ***Seyfullah et al., 2018***).

Our charophyte, palynological, and ostracod data support the dating of the level AR-1 as early Albian age (around 110 Ma), as previously proposed for Ariño and, more generally, the whole Escucha Fm. (***Alcalá et al., 2012; Tibert, 2013; Villanueva-Amadoz et al., 2015; Bover-Arnal et al., 2016; Vajda et al., 2016***). The whole timespan of the co-occurrence of the charophytes *Atopochara trivolvis* var. *trivolvis* and *Clavator harrisii* var. *harrisii* is late Barremian–early Albian. However, in the late Barremian–early Aptian timespan, these species are associated to *A. trivolvis* var. *triquetra* (***Pérez-Cano et al., 2020***). Based on the occurrence of homogeneous populations of *A. trivolvis* var. *trivolvis*, the studied assemblage is assigned to the upper Aptian–lower Albian European Clavator grovesii var. corrugatus (=Clavator grovesii var. lusitanicus) biozone of ***Riveline et al. (1996)***. This view is complementary to that based on the previously found co-occurrence in Ariño of *Clavator harrisii* var. *harrisii* and *Clavator harrisii* var. *zavialensis* indicating an early Albian age (***Tibert et al., 2013***). The oldest occurrence of *A. trivolvis* var. *trivolvis* has recently been reported from the upper Barremian (***Pérez-Cano et al., 2020***), but this variety is more characteristic of upper Aptian–Albian deposits (***Martín-Closas, 2000***).

Regarding the palynomorphs, and in accordance with the age inferred by ***Peyrot et al. (2007)***, the occurrence of *Retimonocolpites dividuus* (***Figure 5—figure supplement 1N***) in ARN-03 indicates an age not older than the late Aptian (***Burden and Hills, 1989***), and the low occurrence of *Tricolpites* sp. (***Figure 5—figure supplement 1P***) indicates a lower Albian age for the studied level (***Tanrikulu et al., 2018***).

The palaeoecological reconstruction of the coastal swamp forest of Ariño that the data herein presented has allowed is remarkably complete. Floristically, the ecosystem was composed of mixed communities of gymnosperms (namely taxodioids and cheirolepids, but also araucariaceans), ferns, and angiosperms as indicated by the palynological assemblages previously obtained (***Villanueva-Amadoz et al., 2015; Vajda et al., 2016***) and the more diverse account presented herein, which is based on larger (or complementary in some aspects) data sampling. Based on coprolite contents, such plants were consumed by the ornithopod and nodosaurid dinosaurs described from the site (***Alcalá et al., 2012; Vajda et al., 2016***). As extant taxodioids are namely comprised of species with a high water requirement, these trees possibly were subjected to periodic flooding similarly to the bald cypress in modern swamps (***Farjon, 2005***). The extinct cheirolepids were encompassed from succulent, shrubby xerophytes to tall forest trees adapted to a wide range of habitats, from coasts to uplands slopes, namely in hot and/or dry climates from lower latitudes (***Anderson et al., 2007***). Moreover, the Ariño swamp local flora was also likely encompassed by anemiacean, dicksoniacean, and/or cyatheacean ferns growing as riparian or in the understorey (***Van Konijnenburg-Van Cittert, 2002***). †Erdtmanithecales, and angiosperms, particularly those of lauralean and chloranthacean affinity, inhabited disturbed and riparian areas (***Doyle et al.,***

644 ***2008***). The diversity of the charophyte and ostracod fauna studied herein is higher
645 than the previously described by ***Tibert et al. (2013)***, which so far can be explained
646 based on palaeoecological constraints, notably the water salinity parameter, or
647 sampling differences. Both charophytes and ostracods lived in shallow permanent
648 water bodies from the freshwater swamp and were well adapted to fluctuating
649 salinities resulting from marine inputs. The presence of the *Theriosynoecum-*
650 *Cypridea-Mantelliana* ostracod association strongly evidences freshwater to slightly
651 saline permanent water bodies (***Horne, 2009***). The intraspecific variability observed
652 on the carapace ornamentation within the *Rosacythere denticulata* specimens is
653 regarded as ecophenotypic (***Sames, 2011***), and could indicate an episodic increase
654 in salinity and/or a variation of salinity, evolving towards brackish conditions.

655 The terrestrial arthropod community of the Ariño swamp forest was very
656 diverse. Spiders, free-roaming or sit-and-wait lurking predators on the forest canopy
657 or floor (***Foelix, 2011***), inhabited the palaeoecosystem, some likely using orbicular
658 webs to hunt the abundant flying insects. The soil-dwelling arthropod fauna consisted
659 of, at least, mites, jumping bristletails, cockroaches, and psocids, all of which were
660 important for nutrient recycling (***Levings and Windsor, 1985***). The finding of a
661 rhagidiid mite (***Figure 4A***) is extraordinary, as the fossil record of this predatory
662 group was limited to a few specimens in Eocene amber (***Judson and Wunderlich,***
663 ***2003***). The Ariño psocid fauna differs from those previously described from other
664 Iberian ambers, and some specimens will be described as new taxa. Extant psocids
665 feed on algae, lichens, and fungi from diverse warm and humid habitats; such
666 autoecology was likely already present in the group during the Cretaceous, rendering
667 them common inhabitants of the resiniferous forests (***Álvarez-Parra et al., 2020b***).
668 The Ariño amber insect groups with phytophagous feeding habits include thrips,

669 hemipterans, and orthopterans. The presence of several thrips as syninclusions
670 could suggest aggregative behaviour. The three aleyrodid hemipterans found are
671 also preserved as syninclusions (***Figure 4I***); the extant relatives of these small sap-
672 sucking insects mostly inhabit angiosperms (***Martin et al., 2000***), contrary to the
673 gymnosperm affinity of the Cretaceous resiniferous trees. Fossil immature
674 thysanopterans are rare, and the Ariño immature specimen could represent an early-
675 stage nymph based on habitus, size, and antennal annulations and microtrichia
676 (***Figure 4B***) (***Vance, 1974***).

677 Holometabolous insects, overwhelmingly diverse and ecologically paramount in
678 modern ecosystems, are well represented in Ariño amber. The exceptional discovery
679 of a lepidopteran caterpillar, very scarce in Cretaceous ambers (***Haug and Haug,***
680 ***2021***) and unprecedented in Iberian amber, implies herbivory not only by adult but
681 also by immature insects in the palaeoecosystem (***Figure 4E***). The two beetle groups
682 tentatively identified, ptinids and cantharids, have been previously found in Iberian
683 amber (***Peris, 2020***). These, according to the habits of extant relatives, are good
684 candidates for having engaged in trophic or even reproductive interactions with
685 plants, as Cretaceous beetles –including some from Iberian amber– are known to
686 have fed on pollen from both gymnosperm and angiosperms, acting as pollinators
687 (***Peris et al., 2020***). The identified dipteran groups presently show various feeding
688 habits, including phytophagy, mycophagy, predation, and ectoparasitism (***McAlpine***
689 ***et al., 1981***). Regarding the latter, female ceratopogonids likely fed on vertebrate
690 blood, probably that from Ariño's dinosaurs according to data from other Iberian
691 ambers (***Pérez-de la Fuente et al., 2011***). As the larval stages and adults of most of
692 the identified dipteran groups chiefly inhabit warm and moist, often aquatic,
693 environments such as diverse wetlands (***McAlpine et al., 1981***), these insects likely

694 thrived in the tropical-subtropical swamp of Ariño. The genus *Burmazelmira* is
695 currently composed of two species from younger ambers; although the discovered
696 *Burmazelmira* sp. male (***Figure 4F***) is similar to *B. grimaldii* from San Just amber
697 (***Arillo et al., 2018***), it shows morphological differences that could warrant describing
698 a new taxon. Lastly, the hymenopteran groups found in Ariño amber are comprised
699 of small to minute forms generally assumed to be idiobiont parasitoids of insect eggs.
700 Platygastroids are the most abundant hymenopterans in Ariño amber, several of
701 them superbly preserved (***Figure 4H***); their predominance is consistent with that
702 observed in other Cretaceous ambers (***Ortega-Blanco et al., 2014***). One
703 mymarommatoid specimen (***Figure 4G***) is similar to *Gallоromma turolensis*
704 (†Gallorommatidae) from San Just amber (***Ortega-Blanco et al., 2011***). The Ariño
705 serphitids and mymarommatoids represent the oldest records worldwide for these
706 groups. The Ariño amber has also yielded vertebrate remains, i.e., the oldest known
707 mammalian hair preserved in amber (***Álvarez-Parra et al., 2020a***) and the
708 pennaceous feather fragment reported herein (***Figure 4J***). These instances
709 showcase the potential of this amber to provide integumentary remains of the
710 vertebrates otherwise preserved as skeleton material in the site's rocks.

711 Considering the extraordinary abundance and diversity of fossils that both the
712 rocks and the amber have yielded, Ariño can be regarded as the most significant
713 locality to date in which fossiliferous amber has been found associated with a
714 dinosaur bonebed (***Figure 6B***). Although the amber palaeodiversity from Fouras/Bois
715 Vert (France) could potentially match that of Ariño (***Perrichot et al., 2007; Tihelka et***
716 ***al., 2021***), the known vertebrate record from Ariño is two orders of magnitude richer,
717 and more complete (***Néraudeau et al., 2003***). The opposite occurs in both the
718 Pipestone Creek (Canada) and the Bone Butte (USA) localities – whereas their

719 vertebrate/dinosaur records are at least comparable (clearly superior for Bone Butte)
720 to those from Ariño, the palaeodiversity described as inclusions from the Ariño amber
721 is one order of magnitude higher, with the fossiliferous potential of the amber
722 probably being significantly greater as well (***Tanke, 2004; Currie et al., 2008; Nel et***
723 ***al., 2010; DePalma, 2010; Cockx et al., 2020***). Indeed, the aerial amber from Ariño
724 stands out for being unusually highly fossiliferous and has already revealed a
725 remarkable diversity in spite of the early stages of its study, including morphotypes
726 that will be described as new taxa. Furthermore, Ariño is the first known locality
727 yielding fossiliferous amber and dinosaur remains in which both elements and the
728 remaining palaeontological assemblage assessed –except some pollen and plant
729 macroremains– generally suffered no or low-grade transport prior to burial
730 (autochthony/parautochthony), and from which amber strictly in situ has been
731 reported for the first time. This has enabled a reliable palaeoecological reconstruction
732 and, more importantly, will keep allowing the extraction of sound palaeoecological
733 inferences from upcoming material. Last but not least, Ariño is the oldest known
734 locality preserving fossiliferous amber in a dinosaur bonebed –the only one hitherto
735 described from the Early Cretaceous–, and it also provides the oldest fossiliferous
736 amber from the Iberian Peninsula. All these characteristics render Ariño one of a
737 kind, offering one of the most complete and integrated pictures from an ancient
738 coastal ecosystem through two diverse and complementary taphonomic windows.
739 This unique ‘dual’ site will remain of interest across many palaeobiological
740 disciplines, and will be of particular significance at promoting studies in emerging
741 fields such as deep-time arthropod-vertebrate interactions.

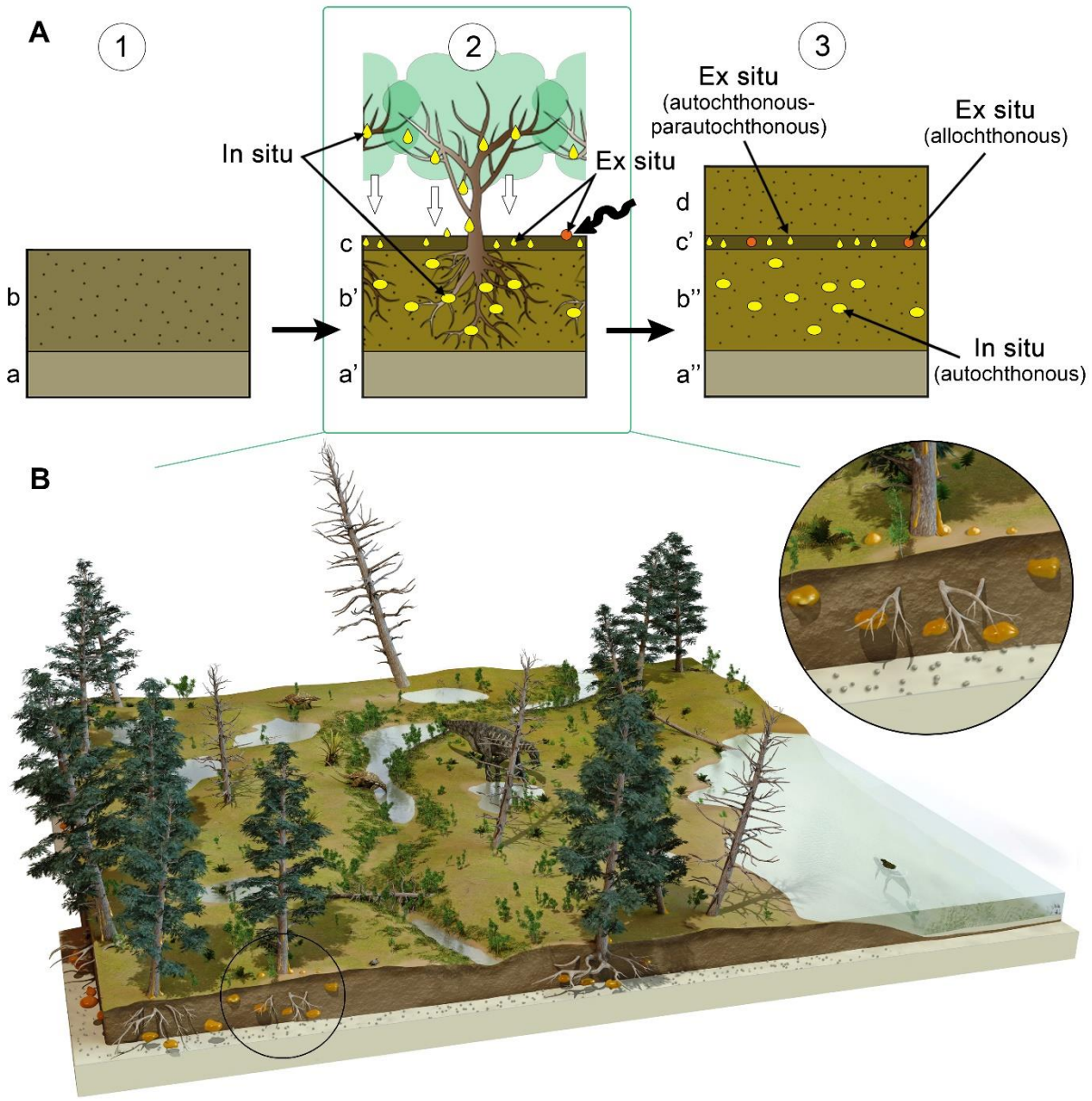

Figure 6. Formation of the amber deposit of Ariño. (**A**) Idealised diagrams depicting (1) the original depositional environment (a, carbonates; b, soil prior to tree installation); (2) resiniferous forest installation and pedogenesis; concentration of in situ kidney-shaped resin pieces produced by the roots in a root horizon (b'); accumulation of aerial resin pieces fallen by gravity from the branches and trunk and a few resin pieces dragged after transport (wavy arrow) in a litter horizon (c); and (3) fossildiagenesis of the resin pieces, resulting in a layer containing strictly in situ autochthonous kidney-shaped amber pieces produced by roots (b''), and a layer

751 mostly composed of strictly ex situ autochthonous-parautochthonous aerial amber
752 pieces and a few potentially allochthonous amber pieces (c'); the level AR-1
753 corresponds to a single cycle of forest floor installation-destruction. (**B**) Artistic
754 reconstruction of the coastal freshwater swamp ecosystem of Ariño, with emphasis
755 on the depositional environment of the resin. The resiniferous trees are
756 araucariaceans (extant model used: *Agathis australis*), tentatively identified as the
757 resin source of Ariño; other depicted terrestrial plants are undetermined vegetation
758 included for artistic purpose. Charophytes and a crocodile (*Hulkepholis plotos*)
759 inhabit the shallow water body on the right; two nodosaurids (*Europelta carbonensis*),
760 an iguanodontian (*Proa valdearinnoensis*), and a turtle (*Aragochersis lignitesta*) are
761 shown on land; these vertebrate species were erected based on the Ariño bonebed
762 material. Artist of the illustration in (B): José Antonio Peñas.
763

764 ## Materials and methods

765

766 ### Fieldwork and material

767 Amber samples were collected from the level AR-1 of the Ariño outcrop in the Santa
768 María open-pit coal mine, near Ariño village (Teruel Province, Aragón, Spain). The
769 amber excavation was carried out in July 2019, after two previous palaeontological
770 amber surveys in July 2018 and May 2019 (permissions 201/10-2018 and 201/10-
771 2019 of the Aragon Government, Spain). Excavation of aerial amber pieces was
772 carried out at two locations from the AR-1 level (***Figure 1C***), near the AR-1/154, AR-
773 1/156, AR-1/157, and AR-1/158 vertebrate concentrations. The acronyms of the
774 amber pieces and bioinclusions are AR-1-A-(number). Field observations on copal
775 associated with *Agathis australis*, herein used for comparison, were conducted at a

776 private propriety in Waipapakauri, close to State Highway 1, North Island of New
777 Zealand, by EP and XD, during a campaign in 2011 and with the permission of the
778 landowner. Macrophotographs of the Ariño site and material were made using a
779 Canon EOS70D.
780
781 **Amber preparation and imaging**
782 Most of the amber pieces with bioinclusions were embedded in epoxy resin (Epo-tek
783 301) following ***Corral et al. (1999)*** to facilitate their preservation and observation.
784 Several amber pieces were cut to observe the fluid inclusions and mineralisations.
785 The amber piece AR-1-A-2019.129 was imaged and analysed with a SEM JEOL
786 6010 PLUS/LA 20 kV with RX (EDS) detector at the Instituto Geológico y Minero de
787 España laboratories (Tres Cantos, Spain). The sample AR-1-A-2018.1 of amber-
788 infilled plant tissue was cleaved in several fragments and thin sections were made to
789 obtain both longitudinal and transversal views of the cellular structure; other non-
790 prepared samples were examined with a Leica Wild M3Z stereozoom microscope,
791 equipped with a x2 frontal lens and a 0.5 to 40 zoom, under tangential light.
792 Microphotographs of the amber inclusions and thin sections of amber-filled plant
793 tissue were made with a sCMEX20 digital camera attached to an Olympus CX41
794 compound microscope taken through ImageFocusAlpha version
795 1.3.7.12967.20180920; images were processed using Photoshop CS6; fine black
796 lines in figures indicate composition of photographs; ***Figure 4C,E,F—figure***
797 ***supplement 1A,G,H*** are formed by stacking. SEM images of amber-infilled plant
798 tissue preserving the cellular structure and charcoalified wood were obtained with a
799 Quanta 200 electronic microscope at the Museo Nacional de Ciencias Naturales
800 (Madrid, Spain). SEM imaging of the amber pieces with taphonomic importance was

carried out with a Quanta 200 electronic microscope at the Scanning Electron Microscopy Unit of the CCiTUB (Universitat de Barcelona); all pieces, except AR-1-A-2019.79, were sputtered with graphite. The amber piece AR-1-A-2019.79 was first submerged in a 50% dissolution of 37% HCl for two minutes and then in distilled water for one day to remove calcium carbonate and gypsum, respectively, from the surface of the piece. The amber piece AR-1-A-2019.93 was carefully unearthed in the field, although a small protruding fragment around 3 cm long was detached. The amber piece and the small fragment were protected to avoid friction on their surface during extraction, transport, and handling. Both were submerged in distilled water for one day. The small fragment was treated with four ultrasonic cleaning cycles of 30 s each; it was placed in a plastic pocket bag with distilled water to avoid friction on its surface. This methodology allows an accurate visualisation of its unaltered surface at the SEM to check if it suffered abrasion.

Amber characterisation

The FTIR (Fourier Transform Infrared Spectroscopy) analyses of the Ariño and San Just ambers were conducted using an IR PerkinElmer Frontier spectrometer that utilises a diamond ATR system with a temperature stabilised DTGS detector and a CsI beam splitter at the Molecular Spectrometry Unit of the CCiTUB. The study of molecular composition and chemotaxonomy was performed after extraction with CH_2Cl_2:CH_3OH (DCM:MeOH 2:1) in a Soxhlet extractor of 2.3858 g of crushed stalactite-type aerial amber pieces, selected for showing the highest transparency and the least possible weathering and inclusion content. After extraction, 1.6126 g of polymeric, organic-insoluble material remained. The crude extract was directly analysed by gas chromatography-mass spectrometry (GC-MS), concentrated to 5 ml

826 at a rotovap, and fractionated using a silica gel column chromatography. Successive
827 elution was performed using n-hexane, n-hexane:DCM 3:1 (fraction 1), DCM (fraction
828 2) and methanol (fraction 3). Fraction 1 contained the aliphatic and tetralin-rich
829 fraction and fraction 2 contained the aromatic fraction, both being analysed by GC-
830 MS after concentration to 1 ml by evaporation in a nitrogen stream. Fraction 3 was
831 dried, forming a creamy white pulverulent residue containing polar terpenoids and
832 resin acids, analysed after conversion to trimethylsilyl derivatives by reaction with
833 N,O-bis-(trimethylsilyl)trifluoroacetamide containing 1% trimethylchlorosilane at 65ºC
834 for 3 h. GC-MS analyses were performed with an Agilent 6850 GC coupled to an
835 Agilent 5975C quadrupole mass spectrometer. Separation was performed on a HP-
836 5MS column coated with (5%-phenyl)-methylpolysiloxane (30 m long, 0.25 mm inner
837 diameter, 0.25 µm film thickness). The operating conditions were as follows: 8 psi He
838 carrier gas pressure, initial temperature hold at 40ºC for 1.5 min, increased from 40
839 to 150ºC at a rate of 15ºC/min, hold for 2 min, increased from 150 to 255ºC at a rate
840 of 5ºC/min, hold isothermal for 20 min, and finally increased to 300ºC at a rate of
841 5ºC/min. The sample was injected in the split mode at 50:1 with the injector
842 temperature at 290ºC. The mass spectrometer was operated in the electron impact
843 mode at an ionisation energy of 70 eV and scanned from 40 to 700 Da. The
844 temperature of the ion source was 230ºC and the quadrupole temperature was
845 150ºC. Data were acquired and processed using the Agilent MassHunter software,
846 and percentages were calculated by normalising the peak areas of the corresponding
847 compounds in the total extracts. Identification of compounds was based on authentic
848 standards and comparison of mass spectra with standard libraries and literature.
849
850 **Charophytes and ostracods**

They were obtained from the level AR-1 after picking the rock associated with the amber. The acronyms of the charophytes and ostracods are AR-1-CH-(number) and AR-1-OS-(number), respectively. The microfossil preparation followed standard methods in micropalaeontology as applied to charophytes (***Pérez-Cano et al., 2020***). Scanning Electron Microscope (SEM) images of selected charophyte and ostracod specimens were obtained using the Quanta 200 scanning electron microscope at the Scanning Electron Microscopy Unit of the CCiTUB. Additional SEM images of ostracods were obtained using a JEOL 6400 device at the Faculty of Earth Sciences, Geography and Astronomy, University of Vienna (Austria). Clavatoracean utricular nomenclature follows that of ***Grambast (1968)***.

Palynology

Four consecutive samples from the level AR-1 (ARN-01–ARN-04) were prepared for palynological studies by the Geologischer Dienst NRW (Germany) (www.gd.nrw.de). ARN-01 and ARN-02 were obtained from the lower (root) layer rich in kidney-shaped amber pieces (ARN-02 closer to the upper layer), and ARN-03 and ARN-04 were gathered from the upper (litter) layer rich in aerial amber pieces (***Figure 1B***). The rock samples were treated following standard palynological preparation techniques (***Traverse, 2007***) consisting of acid attack with HCl, HF, and diluted HNO_3 and sieving with different grid sizes (500, 250, 75, 50, and 12 µm). Samples were studied with an Olympus BX51 brightfield light microscope attached to a ColorView IIIu camera. The percentage ranges provided in the results show the lowest and the highest abundance of the corresponding taxon in the four samples.

Material availability

All the material obtained prior and during the amber excavation in Ariño is housed at the Museo Aragonés de Paleontología (Fundación Conjunto Paleontológico de Teruel-Dinópolis, Teruel Province, Spain).

The copal pieces for comparison are housed at the Museo Geominero of the Instituto Geológico y Minero de España (IGME) and Universitat de Barcelona (UB).

Acknowledgements

We are grateful to the SAMCA Group for its collaboration. We thank the permissions of the Dirección General de Patrimonio Cultural del Gobierno de Aragón (Spain) to excavate. We thank Alejandro Gallardo (Laboratory of Palaeontology-UB), Telm Bover-Arnal (UB), Guillermo Rey, José Antonio Peñas, and the technicians of the CCiTUB. Equipment has been partly funded by FEDER (IGME13-4E-1518). We are grateful to the Departamento de Ciencia, Innovación y Sociedad del Conocimiento, Gobierno de Aragón (Grupo de Investigación de Referencia E04_20R) y Ministerio de Ciencia e Innovación, Gobierno de España (Unidad de Paleontología de Dinosaurios de Teruel and AMBERIA Team). This study is a contribution to the projects CRE CGL2017-84419, PGC2018-094034-B-C22 (both from the Ministerio de Ciencia, Innovación y Universidades, Spain, AEI/FEDER, UE), BIOGEOEVENTS CGL2015-69805-P (Ministerio de Economía y Competitividad, Spain, and the European Regional Development Fund), 2017SGR-824 (AGAUR, Generalitat de Catalunya, Spain), UNESCO IGCP Project 661 of the Austrian Academy of Sciences, and LR18 ES07 (Faculty of Sciences, Université de Tunis El Manar). J.P.-C. acknowledges the support from the Ministerio de Economía y Competitividad (BES-2016-076469). A.S.-G. is funded by an APOSTD2019 Research Fellowship (Generalitat Valenciana, Spain) and the European Social Fund. R.P.-d.l.F. is funded

by a Research Fellowship (Oxford University Museum of Natural History, UK). This study forms part of the first author's (S.Á.-P.) doctoral thesis, supported by a grant from the Secretaria d'Universitats i Recerca de la Generalitat de Catalunya and the European Social Fund (2020FI_B1 00002).

Additional information

Funding

Funder	Grant reference number	Author
Ministerio de Ciencia, Innovación y Universidades (Spain)	CGL2017-84419	Xavier Delclòs and Eduardo Barrón
Ministerio de Ciencia, Innovación y Universidades (Spain)	PGC2018-094034-B-C22	Luis Alcalá
Ministerio de Economía y Competitividad (Spain) and the European Regional Development Fund	CGL2015-69805-P	Carles Martín-Closas
AGAUR, Generalitat de Catalunya (Spain)	2017SGR-824	Xavier Delclòs
Secretaria d'Universitats i Recerca de la Generalitat	2020FI_B1 00002	Sergio Álvarez-Parra

de Catalunya and the European Social Fund		
Research Fellowship (Oxford University Museum of Natural History, UK)		Ricardo Pérez-de la Fuente
Ministerio de Economía y Competitividad (Spain)	BES-2016-076469	Jordi Pérez-Cano
UNESCO IGCP of the Austrian Academy of Sciences (Austria)	Project 661	Khaled Trabelsi
Research fellowship (Faculty of Sciences, Université de Tunis El Manar, Tunisia)	LR18 ES07	Khaled Trabelsi
Generalitat Valenciana (Spain)	APOSTD2019	Alba Sánchez-García
European Regional Development Fund	IGME13-4E-1518	Rafael P Lozano

The funders had no role in study design, data collection and interpretation, or the decision to submit the work for publication.

Author contributions

Sergio Álvarez-Parra, Conceptualisation, Fieldwork, Investigation, Methodology, Supervision, Writing – original draft, Writing – review and editing; Ricardo Pérez-de la Fuente, Conceptualisation, Fieldwork, Investigation, Writing – original draft, Writing – review and editing; Enrique Peñalver: Conceptualisation, Fieldwork, Investigation, Supervision, Writing – review and editing; Eduardo Barrón, Fieldwork, Investigation, Methodology, Project administration; Luis Alcalá, Fieldwork, Investigation, Project administration; Jordi Pérez-Cano, Investigation, Methodology; Carles Martín-Closas, Investigation, Methodology; Khaled Trabelsi, Investigation, Methodology; Nieves Meléndez, Fieldwork, Investigation, Methodology; Rafael López Del Valle, Fieldwork, Methodology; Rafael P Lozano, Fieldwork, Investigation, Methodology; David Peris, Fieldwork, Investigation; Ana Rodrigo, Fieldwork; Víctor Sarto i Monteys, Fieldwork; Carlos A Bueno-Cebollada, Investigation; César Menor-Salván, Investigation, Methodology; Marc Philippe, Investigation, Methodology; Alba Sánchez-García, Investigation; Constanza Peña-Kairath, Fieldwork; Antonio Arillo, Investigation; Eduardo Espílez, Fieldwork, Investigation; Luis Mampel, Fieldwork, Investigation; Xavier Delclòs, Conceptualisation, Fieldwork, Investigation, Project administration, Supervision, Writing – review and editing. All authors contributed to the discussion.

Author ORCIDs

Sergio Álvarez-Parra: https://orcid.org/0000-0002-0232-1647

Ricardo Pérez-de la Fuente: https://orcid.org/0000-0002-2830-2639

Enrique Peñalver: https://orcid.org/0000-0001-8312-6087

Eduardo Barrón: https://orcid.org/0000-0003-4979-1117

Luis Alcalá: https://orcid.org/0000-0002-6369-6186

Jordi Pérez-Cano: https://orcid.org/0000-0002-1782-5346

Carles Martín-Closas: https://orcid.org/0000-0003-4349-738X

Khaled Trabelsi: https://orcid.org/0000-0003-0207-9819

Nieves Meléndez: https://orcid.org/0000-0002-9476-740X

Rafael López Del Valle: https://orcid.org/0000-0002-7164-9558

Rafael P Lozano: https://orcid.org/0000-0002-1022-3860

David Peris: https://orcid.org/0000-0003-4074-7400

Ana Rodrigo: https://orcid.org/0000-0001-7201-9286

Víctor Sarto i Monteys: https://orcid.org/0000-0003-2701-6558

Carlos A Bueno-Cebollada: https://orcid.org/0000-0003-0367-4177

César Menor-Salván: https://orcid.org/0000-0002-1238-190X

Marc Philippe: https://orcid.org/0000-0002-4658-617X

Alba Sánchez-García: https://orcid.org/0000-0003-0911-2001

Constanza Peña-Kairath: https://orcid.org/0000-0002-4877-7754

Antonio Arillo: https://orcid.org/0000-0002-4878-5797

Eduardo Espílez: https://orcid.org/0000-0002-9794-1776

Luis Mampel: https://orcid.org/0000-0002-0329-7319

Xavier Delclòs: https://orcid.org/0000-0002-2233-5480

Declaration of interests

The authors declare no competing interests.

Additional files

Supplementary files

965 **Supplementary Video 1.** Amber excavation in the lower Albian bonebed level AR-1
966 of Ariño during May 2019 and extraction of two strictly in situ (autochthonous) kidney-
967 shaped amber pieces from the root layer. See also ***Figures 1 and 2***.

968

969 **Supplementary Table 1. List of palynomorphs recorded from the lower Albian**
970 **bonebed level AR-1 of Ariño and their relative abundances.** ARN-01 and ARN-02
971 were obtained from the lower root layer with kidney-shaped amber pieces, and ARN-
972 03 and ARN-04 from the upper litter layer rich in aerial amber pieces, all of them
973 within the level AR-1. See also ***Figure 5—figure supplement 1***.

974

975 **Figure 3—source data 1.** FTIR data of the Ariño amber 1.

976

977 **Figure 3—source data 2.** FTIR data of the Ariño amber 2.

978

979 **Figure 3—source data 3.** FTIR data of the San Just amber.

980

981 **Figure 3—source data 4.** GC-MS data of the Ariño amber.

982

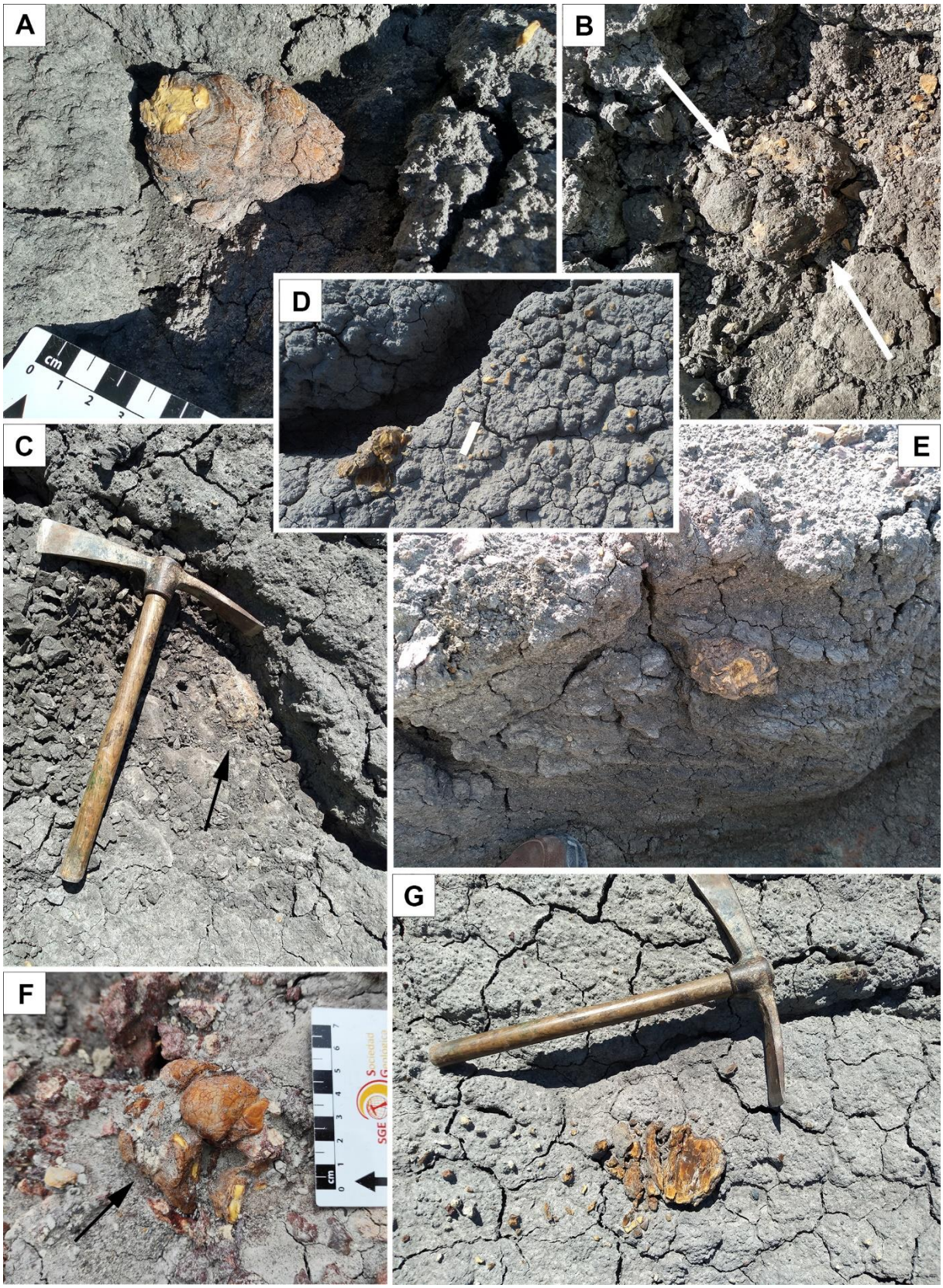

Figure 2—figure supplement 1. Strictly in situ (autochthonous) kidney-shaped amber pieces from the root layer of the lower Albian bonebed level AR-1 of Ariño. (**A**)

Slightly elongate piece exposed by the weathering, but not moved, lacking a detached small surface fragment (left). (**B**, **C**) Two rounded and slightly elongate pieces (white arrows in (B) and black arrow in (C)) partially exposed during excavation (piece diameter in (B) = 9 cm; pickaxe length in (C) = 35 cm). (**D**) Strictly in situ piece fragmented by the weathering, and fragments of another piece on the right (paper strip = 4 cm). (**E**) Piece partially exposed in the sidewall of a small gully excavated by rain (piece diameter = ca. 7.5 cm). (**F**) Irregular in situ piece indicated with an arrow; centimetric scale. (**G**) Crumbled amber piece (pickaxe length = 35 cm). (D, E) excavated during July 2018 and the rest during May 2019.

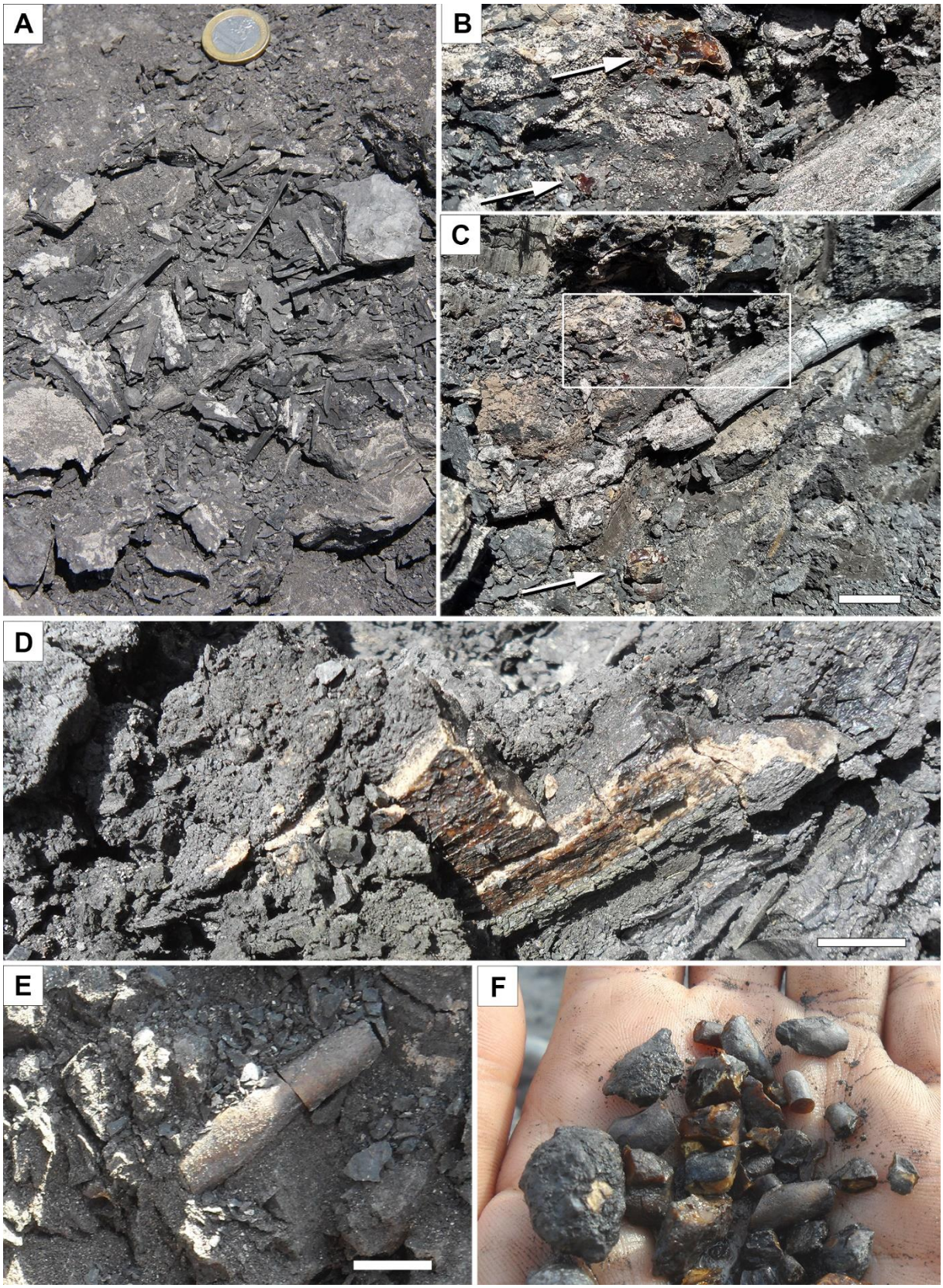

Figure 2—figure supplement 2. Litter layer of the lower Albian bonebed level AR-1 of Ariño. (**A**) Plant remains, most likely elongate charcoalified wood pieces (coin

diameter = 2.3 cm). (**B**, **C**) Strictly ex situ (autochthonous) aerial amber pieces (arrows) and elongate woody remains ((B) is the enlarged inset in (C)). (**D**) Strictly ex situ flattened amber piece most likely originated from resin coating the trunk or infilling a broken trunk. (**E**) Strictly ex situ stalactite-shaped aerial amber piece. (**F**) Assortment of aerial amber piece fragments. (A, D–F) excavated during July 2019 and the rest during May 2019. Scale bars, 2 cm (C), and 1 cm (D, E).

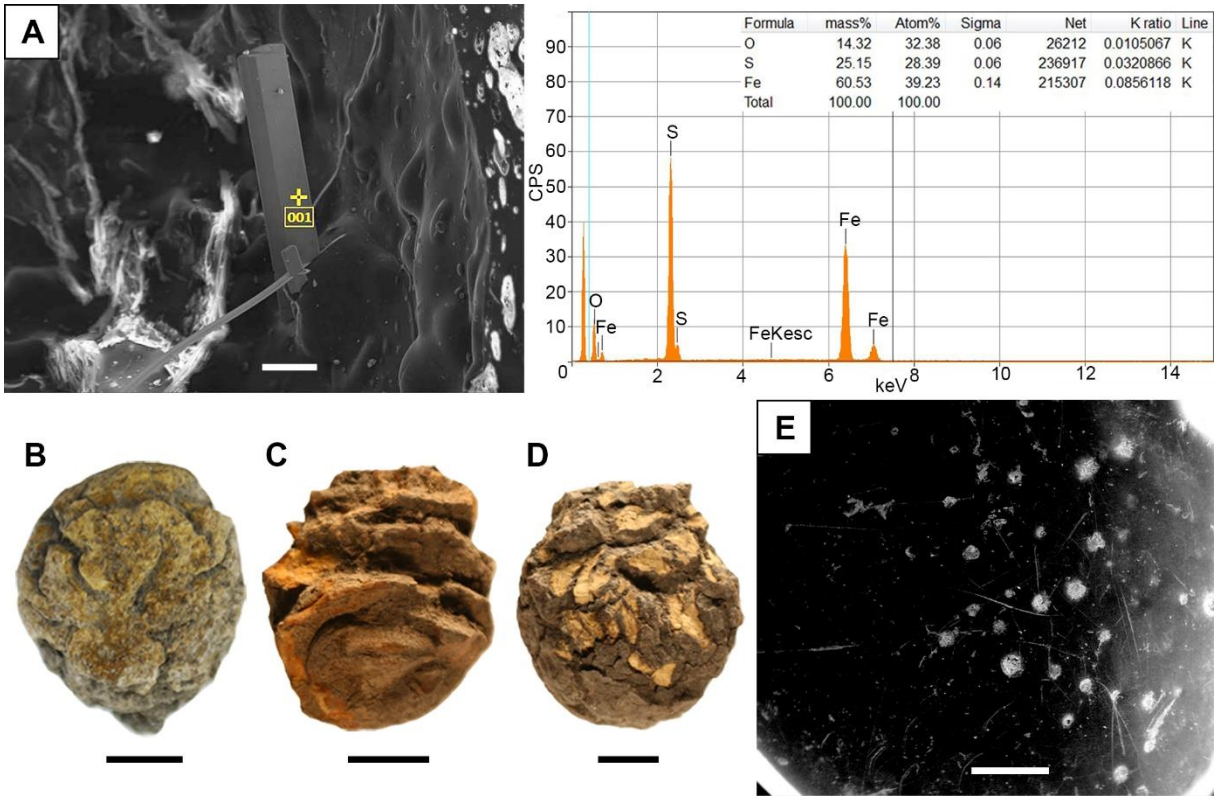

Figure 2—figure supplement 3. Amber pieces with taphonomic interest from the level AR-1 of Ariño. (**A**) EDS analysis of the needle-shaped crystals from an iron sulphate (likely szomolnokite) growing inward from the walls in the alleged empty space left by a fluid bubble-like inclusion of an amber piece (AR-1-A-2019.129). (**B**–**D**) Small, almost spherical amber masses from the litter layer (AR-1-A-2019.131, AR-1-A-2019.132 and AR-1-A-2019.133, respectively). (**E**) Surface of a peculiar amber

1013 piece found in the litter layer, showing surface borings and linear grooves (AR-1-A-
1014 2019.79). Scale bars, 0.1 mm (A), 5 mm (B), 1 cm (C, D), and 1 mm (E).
1015

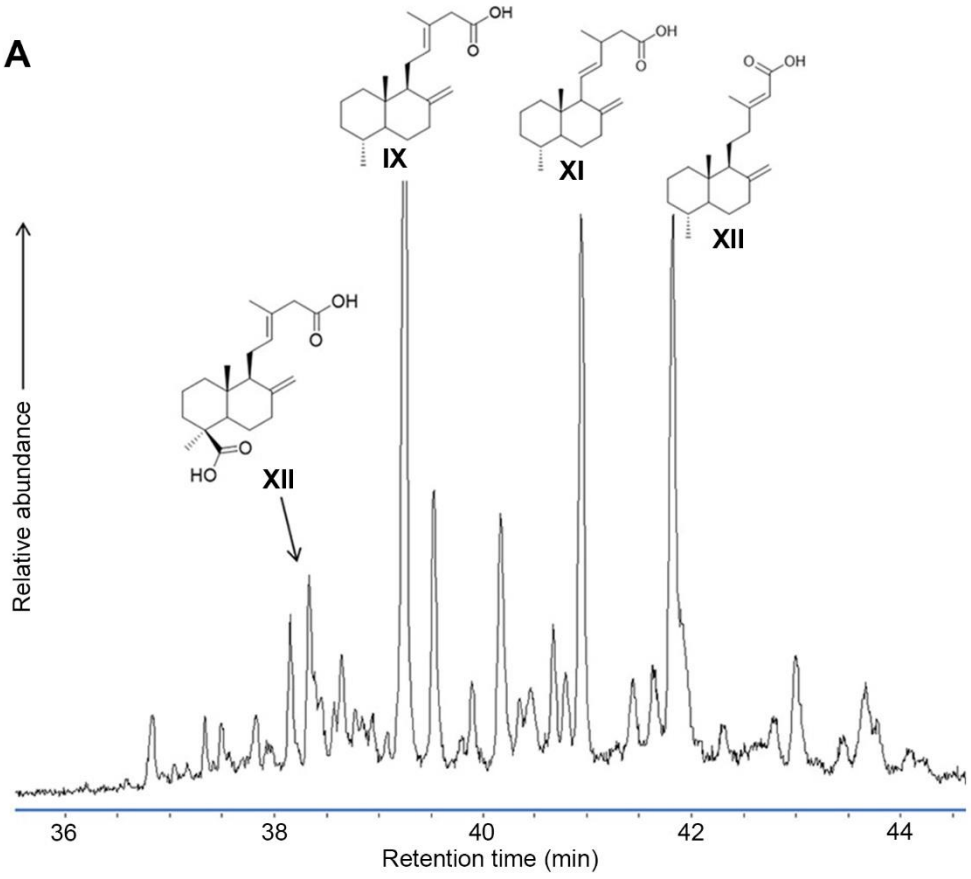

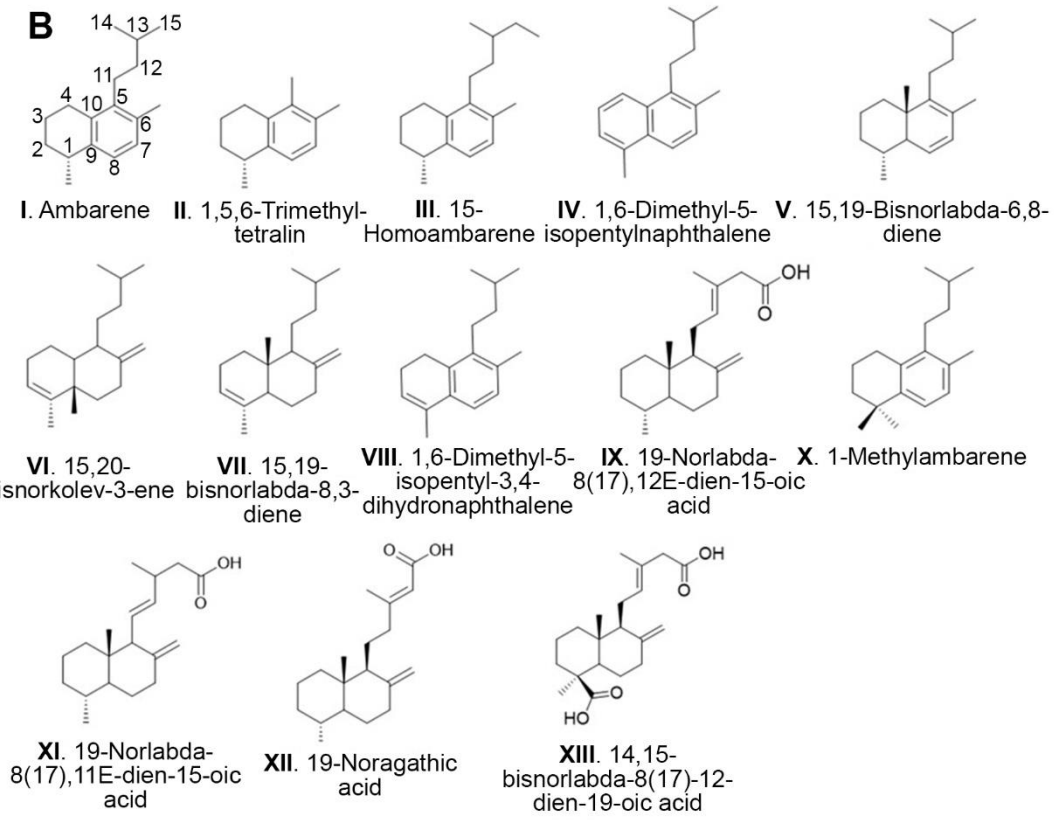

1016

1017 **Figure 3—figure supplement 1.** Physicochemical characterisation of the Lower
1018 Cretaceous amber from Ariño. (**A**) Gas chromatography-mass spectrometry (GC-MS)
1019 chromatogram corresponding to the polar fraction of the organic extract of the Ariño
1020 amber, showing labdanoic acids as main components; decarboxylation and
1021 disproportionation of labdanoic acids lead to the main hydrocarbons found,
1022 diterpenes of the labdane family. (**B**) Chemical structures cited in the work.
1023

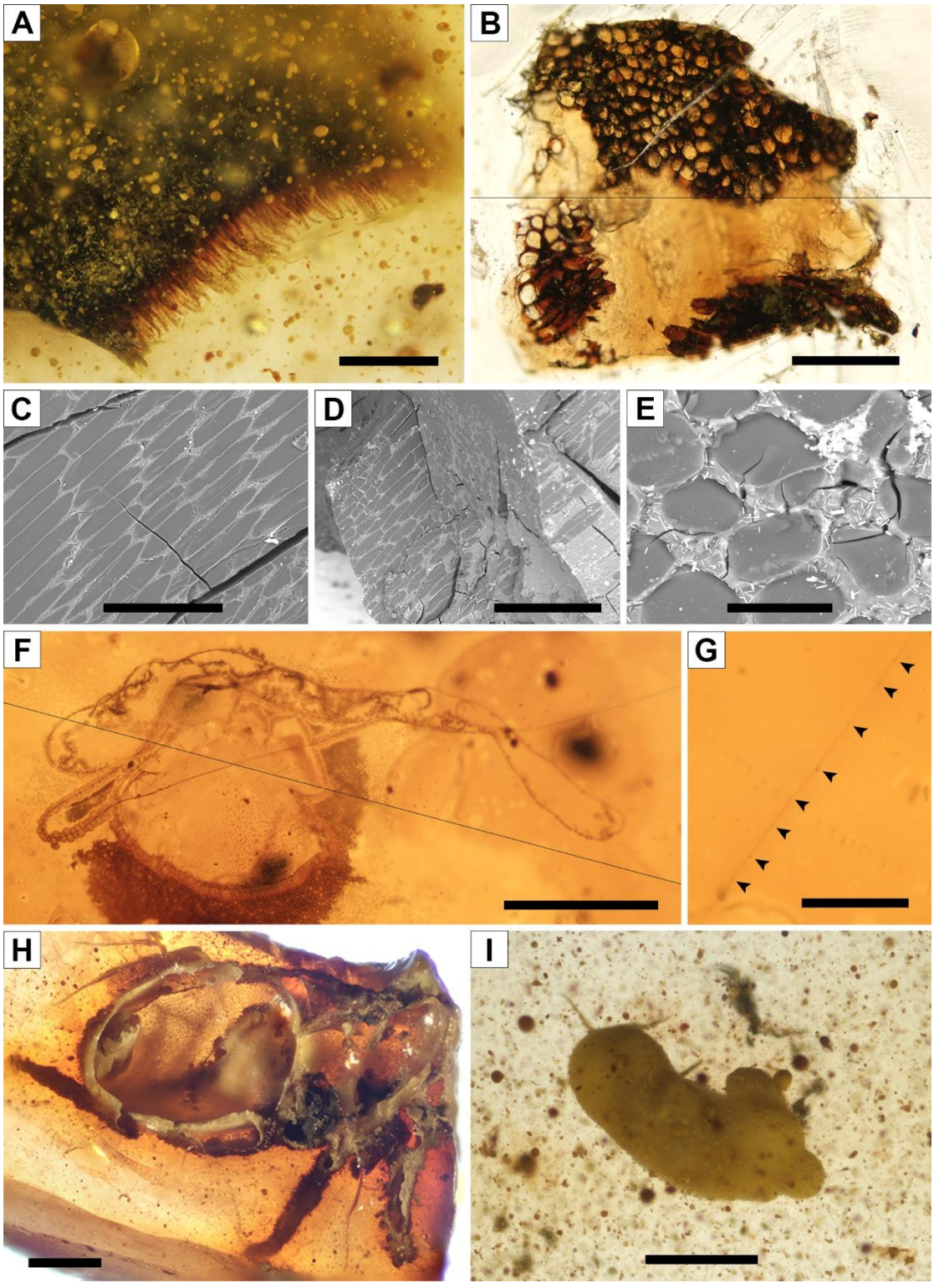

Figure 4—figure supplement 1. Diverse bioinclusions in amber from the level AR-1 of Ariño. (**A**) Plant remain (AR-1-A-2019.114.3). (**B**–**E**) Amber-infilled plant tissue preserving the cellular structure that could correspond to suber (cork) (AR-1-A-2018.1): (**B**) Preparation (transversal view); (**C**–**E**) SEM images: (**C**) in longitudinal

1029 and oblique view, (**D**) in transversal and oblique view, and (**E**) in transversal view. (**F**)
1030 A tangled spiderweb portion (AR-1-A-2019.95.5). (**G**) Detail photograph of a
1031 spiderweb strand found in the former, with glue droplets marked with arrowheads. (**H**)
1032 Spider showing the inner body structure in the surface of a broken amber piece (AR-
1033 1-A-2019.76). (**I**) Thrips showing a thin milky coat (AR-1-A-2019.114.1). Scale bars,
1034 0.2 mm (A, C), 0.5 mm (B, F, H, I), 0.3 mm (D), 0.02 mm (E), and 0.05 mm (G).
1035

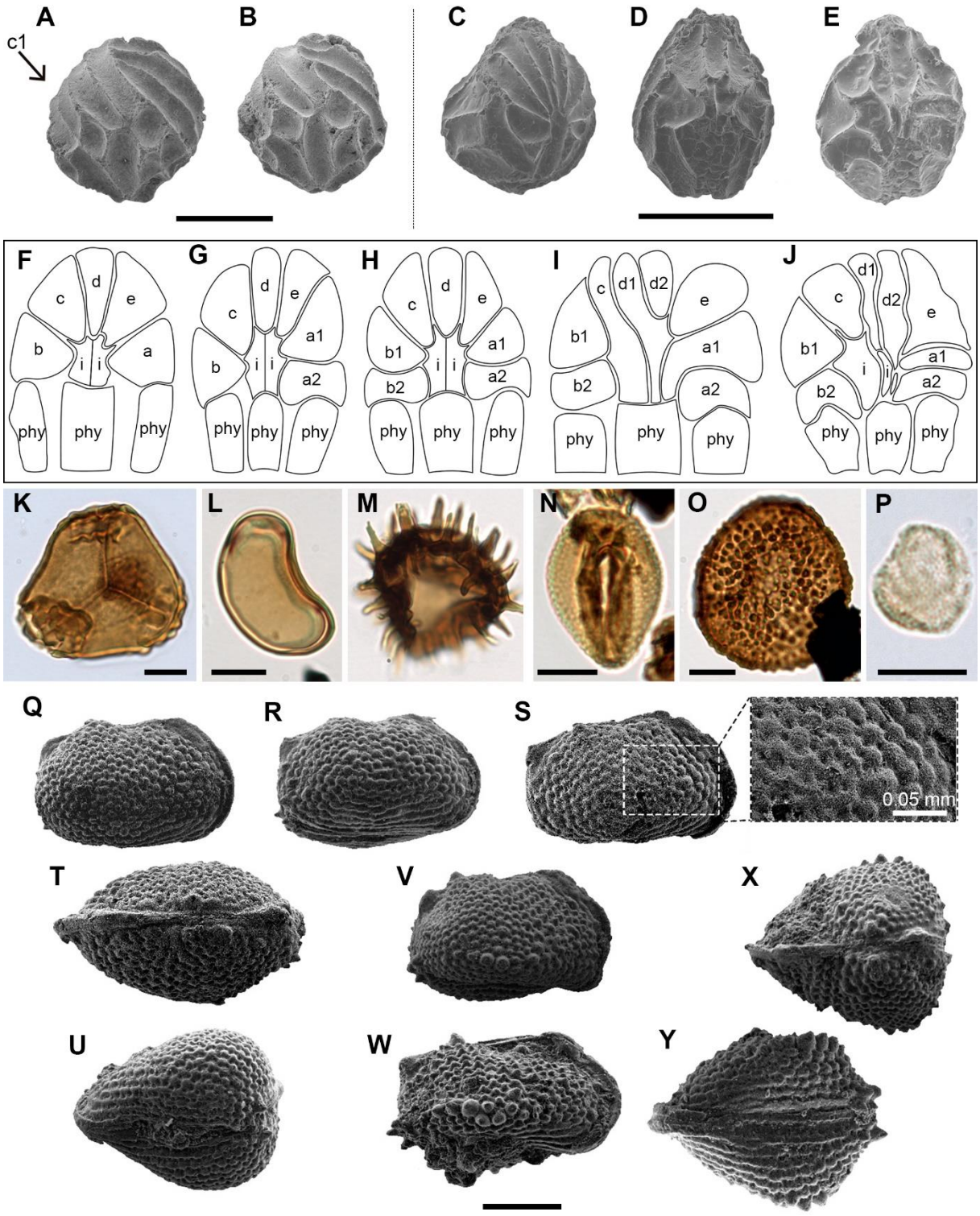

Figure 5—figure supplement 1. Additional charophyte (A–J), palynomorph (K–P), and ostracod (Q–Y) records sampled from level AR-1 of Ariño. (**A**, **B**) *Atopochara trivolvis* var. *trivolvis* (†Clavatoraceae) lateral views (AR-1-CH-003 and AR-1-CH-006, respectively); cell lettering after ***Grambast (1968)***. (**C**–**E**) *Clavator harrisii* var.

harrisii (†Clavatoraceae): (**C**) Lateral view (AR-1-CH-010); (**D**) Abaxial view morphotype I (AR-1-CH-012); (**E**) Abaxial view morphotype V (AR-1-CH-016). (**F**–**J**) Morphotypes of the abaxial part of the utricle of *Clavator harrisii* var. *harrisii*: (**F**) Morphotype I showing the impression of the phylloid cortical cells (phy), two intermediate cells (i) and an adaxial fan with five cells, two lateral cells (a and b) and three apical cells (c, d, e); (**G**) Morphotype II showing the adaxial fan with six cells by subdivision of the a cell; (**H**) Morphotype III showing the adaxial fan with seven cells by subdivision of a and b cells; (**I**) Morphotype IV showing an adaxial fan with eight cells by subdivision of d cell in addition to the other subdivisions already found in morphotype II, fusion of fan cells and intermediate cells is also observed; (**J**) Morphotype V with the same number of fan cells as in morphotype IV but showing different cell shapes and no fusion between intermediate and fan cells. (**K**) *Trilobosporites purverulentus* (ARN-02). (**L**) *Laevigatosporites haardti* (ARN-01). (**M**) *Ceratosporites* sp. (ARN-02). (**N**) *Retimonocolpites dividuus* (ARN-03). (**O**) *Foraminisporis* cf. *undulatus* (ARN-01). (**P**) *Tricolpites* sp. (ARN-04). (**Q**–**Y**) *Rosacythere denticulata* (Limnocytheridae): (**Q**–**U**) Variant with well-developed rosette ornamentation: (**Q**–**S**) Female carapaces, right lateral views and detail of the ornamentation (AR-1-OS-008, AR-1-OS-009 and AR-1-OS-010, respectively); (**T**) Male carapace, dorsal view (AR-1-OS-013); (**U**) Female carapace, ventral view (AR-1-OS-014); (**V**–**Y**) Variant with well-developed rosette ornamentation and spine-like node: (**V**, **W**) Female and male carapace respectively, right lateral views (AR-1-OS-016 and AR-1-OS-017, respectively); (**X**) Female carapace, dorsal view (AR-1-OS-019); (**Y**) Female carapace, ventral view (AR-1-OS-20). Scale bars, 0.05 mm (A–E), 0.01 mm (K–P), and 0.2 mm (Q–Y).

1066 **Data availability**

1067 All data generated or analysed during this study are included in the manuscript and
1068 supporting files. Palynomorphs taxa and their abundances are available in
1069 ***Supplementary Table 1***. Source data of FTIR analyses are available in **Figure 3—**
1070 **source *data 1–3***. Source data of GC-MS are available in **Figure 3—source *data 4***.

1071

1072 ## References

1073

1074 Alcalá L, Espílez E, Mampel L, Kirkland JI, Ortiga M, Rubio D, González A, Ayala D,
1075 Cobos A, Royo-Torres R, Gascó F, Pesquero MD. 2012. A new Lower Cretaceous
1076 vertebrate bonebed near Ariño (Teruel, Aragón, Spain); found and managed in a
1077 joint collaboration between a mining company and a palaeontological park.
1078 *Geoheritage* **4**:275–286. DOI: https://doi.org/10.1007/s12371-012-0068-y

1079 Alcalá L, Espílez E, Mampel L. 2018. Ariño: La mina de los dinosaurios. In: Zamora S
1080 (Ed), *Fósiles: Nuevos Hallazgos Paleontológicos en Aragón*. Zaragoza, Spain:
1081 Institución «Fernando el Católico», pp. 111–141.

1082 Allison PA. 1990. Diagenesis. Pyrite. In: Briggs DEG, Crowther PR (Eds),
1083 *Palaeobiology: A synthesis*. Hoboken, USA: Blackwell Science, pp. 253–255.

1084 Alonso J, Arillo A, Barrón E, Corral JC, Grimalt J, López JF, López R, Martínez-
1085 Delclòs X, Ortuño V, Peñalver E, Trincão PR. 2000. A new fossil resin with
1086 biological inclusions in Lower Cretaceous deposits from Álava (northern Spain,
1087 Basque-Cantabrian Basin). *Journal of Paleontology* **74**:158–178. DOI:
1088 https://doi.org/10.1017/S0022336000031334

1089 Álvarez-Parra S, Delclòs X, Solórzano-Kraemer MM, Alcalá L, Peñalver E. 2020a.
1090 Cretaceous amniote integuments recorded through a taphonomic process unique

1091 to resins. *Scientific Reports* **10**:19840. DOI: https://doi.org/10.1038/s41598-020-
1092 76830-8
1093 Álvarez-Parra S, Peñalver E, Nel A, Delclòs X. 2020b. The oldest representative of
1094 the extant barklice genus *Psyllipsocus* (Psocodea: Trogiomorpha: Psyllipsocidae)
1095 from the Cenomanian amber of Myanmar. *Cretaceous Research* **113**:104480.
1096 DOI: https://doi.org/10.1016/j.cretres.2020.104480
1097 Anderson JA, Anderson HM, Cleal CJ. 2007. *Brief History of the Gymnosperms:*
1098 *Classification, Biodiversity, Phytogeography and Ecology*. Pretoria, South Africa:
1099 South African National Biodiversity Institute.
1100 Arillo A, Blagoderov V, Peñalver E. 2018. Early Cretaceous parasitism in amber: A
1101 new species of *Burmazelmira* fly (Diptera: Archizelmiridae) parasitized by a *Leptus*
1102 sp. mite (Acari, Erythraeidae). *Cretaceous Research* **86**:24–32. DOI:
1103 https://doi.org/10.1016/j.cretres.2018.02.006
1104 Bell PR, Currie PJ. 2016. A high-latitude dromaeosaurid, *Boreonykus certekorum*,
1105 gen. et sp. nov. (Theropoda), from the upper Campanian Wapiti Formation, west-
1106 central Alberta. *Journal of Vertebrate Paleontology* **36**:e1034359. DOI:
1107 https://doi.org/10.1080/02724634.2015.1034359
1108 Bover-Arnal T, Moreno-Bedmar JA, Frijia G, Pascual-Cebrian E, Salas R. 2016.
1109 Chronostratigraphy of the Barremian–Early Albian of the Maestrat Basin (E Iberian
1110 Peninsula): integrating strontium-isotope stratigraphy and ammonoid
1111 biostratigraphy. *Newsletters on Stratigraphy* **49**:41–68. DOI:
1112 https://doi.org/10.1127/nos/2016/0072
1113 Burden ET, Hills LV. 1989. Illustrated key to genera of Lower Cretaceous terrestrial
1114 palynomorphs (excluding megaspores) of Western Canada. *American Association*
1115 *of Stratigraphic Palynologists Foundation, Contribution Series* **21**:1–147.

1116 Buscalioni ÁD, Alcalá L, Espílez E, Mampel L. 2013. European Goniopholididae from
1117 the Early Albian Escucha Formation in Ariño (Teruel, Aragón, Spain). *Spanish*
1118 *Journal of Palaeontology* **28**:103–122. DOI: https://doi.org/10.7203/sjp.28.1.17835
1119 Cervera A, Pardo G, Villena J. 1976. Algunas precisiones litoestratigráficas sobre la
1120 formación 'Lignitos de Escucha'. *Tecniterrae* **14**:25–33.
1121 Cockx P, McKellar R, Tappert R, Vavrek M, Muehlenbachs K. 2020. Bonebed amber
1122 as a new source of paleontological data: The case of the Pipestone Creek deposit
1123 (Upper Cretaceous), Alberta, Canada. *Gondwana Research* **81**:378–389. DOI:
1124 https://doi.org/10.1016/j.gr.2019.12.005
1125 Cockx P, Tappert R, Muehlenbachs K, Somers C, McKellar R. 2021. Amber from a
1126 *Tyrannosaurus rex* bonebed (Saskatchewan, Canada) with implications for
1127 paleoenvironment and paleoecology. *Cretaceous Research* **125**:104865. DOI:
1128 https://doi.org/10.1016/j.cretres.2021.104865
1129 Corral JC, López Del Valle R, Alonso J. 1999. El ámbar cretácico de Álava (Cuenca
1130 Vasco-Cantábrica, norte de España). Su colecta y preparación. *Estudios del*
1131 *Museo de Ciencias Naturales de Álava* **14**:7–21.
1132 Cox RE, Yamamoto S, Otto A, Simoneit BRT. 2007. Oxygenated di- and tricyclic
1133 diterpenoids of southern hemisphere conifers. *Biochemical Systematics and*
1134 *Ecology* **35**:342–362. DOI: https://doi.org/10.1016/j.bse.2006.09.013
1135 Currie PJ, Langston WJr, Tanke DH. 2008. *A New Horned Dinosaur from an Upper*
1136 *Cretaceous Bonebed in Alberta*. Ottawa, Canada: NRC Research Press.
1137 Delclòs X, Arillo A, Peñalver E, Barrón E, Soriano C, López Del Valle R, Bernárdez,
1138 E, Corral C, Ortuño VM. 2007. Fossiliferous amber deposits from the Cretaceous
1139 (Albian) of Spain. *Comptes Rendus Palevol* **6**:135–149. DOI:
1140 https://doi.org/10.1016/j.crpv.2006.09.003

1141 Delclòs X, Peñalver E, Ranaivosoa V, Solórzano-Kraemer MM. 2020. Unravelling the
1142 mystery of “Madagascar copal”: Age, origin and preservation of a Recent resin.
1143 *PLoS One* **15**:e0232623. DOI: https://doi.org/10.1371/journal.pone.0232623
1144 DePalma RA. 2010. *Geology, taphonomy, and paleoecology of a unique Upper*
1145 *Cretaceous bonebed near the Cretaceous-Tertiary boundary in South Dakota*:
1146 PhD Dissertation, University of Kansas.
1147 DePalma R, Cichocki F, Dierick M, Feeney R. 2010. Preliminary notes on the first
1148 recorded amber insects from the Hell Creek Formation. *The Journal of*
1149 *Paleontological Sciences*, C.10.0001.
1150 DePalma RA, Burnham DA, Martin LD, Larson PL, Bakker RT. 2015. The first giant
1151 raptor (Theropoda: Dromaeosauridae) from the Hell Creek
1152 Formation. *Paleontological Contributions* **14**:1–16. DOI:
1153 https://doi.org/10.17161/paleo.1808.18764
1154 Doyle JA, Endress PK, Upchurch GR. 2008. Early Cretaceous monocots: a
1155 phylogenetic evaluation. *Acta Musei Nationalis Pragae series B - Historia Naturalis*
1156 **64**:59–87. DOI: https://doi.org/10.5167/uzh-11654
1157 Farjon A. 2005. *A monograph of Cupressaceae and* Sciadopitys. London, UK: Royal
1158 Botanic Gardens.
1159 Foelix RF. 2011. *Biology of Spiders*. Oxford, UK: Oxford University Press.
1160 Girard V, Breton G, Perrichot V, Bilotte M, Le Loeuff J, Nel A, Philippe M, Thevenard
1161 F. 2013. The Cenomanian amber of Fourtou (Aude, Southern France): Taphonomy
1162 and palaeoecological implications. *Annales de Paléontologie* **99**:301–315. DOI:
1163 https://doi.org/10.1016/j.annpal.2013.06.002
1164 Grambast L. 1968. Evolution of the utricle in the charophyta genera *Perimneste*
1165 Harris and *Atopochara* Peck. *Journal of the Linnean Society (Botany)* **61**:5–11.

1166 Grimaldi DA, Engel MS, Nascimbene PC. 2002. Fossiliferous Cretaceous amber
1167 from Myanmar (Burma): its rediscovery, biotic diversity, and paleontological
1168 significance. *American Museum Novitates* **3361**:1–71. DOI:
1169 https://doi.org/10.1206/0003-0082(2002)361<0001:FCAFMB>2.0.CO;2
1170 Grimalt JO, Simoneit BRT, Hatcher PG, Nissenbaum A. 1988. The molecular
1171 composition of ambers. *Organic Geochemistry* **13**:677–690. DOI:
1172 https://doi.org/10.1016/0146-6380(88)90089-7
1173 Haug JT, Haug C. 2021. A 100 million-year-old armoured caterpillar supports the
1174 early diversification of moths and butterflies. *Gondwana Research* **93**:101–105.
1175 DOI: https://doi.org/10.1016/j.gr.2021.01.009
1176 Henwood A. 1993. Recent plant resins and the taphonomy of organisms in amber: a
1177 review. *Modern Geology* **19**:35−59.
1178 Horne DJ. 2009. Purbeck–Wealden. In: Whittaker JE, Hart MB (Eds), *Ostracods in*
1179 *British Stratigraphy*. London, UK: The Geological Society of London, pp. 289–308.
1180 Judson M, Wunderlich J. 2003. Rhagidiidae (Acari, Eupodoidea) from Baltic amber.
1181 *Acta Zoologica Cracoviensia* **46**:147–152.
1182 Kawamura T, Koshino H, Nakamura T, Nagasawa Y, Nanao H, Shirai M, Uesugi S,
1183 Ohno M, Kimura K. 2018. Amberene and 1-methylamberene, isolated and
1184 identified from Kuji amber (Japan). *Organic Geochemistry* **120**:12–18. DOI:
1185 https://doi.org/10.1016/j.orggeochem.2018.02.014
1186 Kirkland JI, Alcalá L, Loewen MA, Espílez E, Mampel L, Wiesma JP. 2013. The basal
1187 nodosaurid ankylosaur *Europelta carbonensis* n. gen., n. sp. from the Lower
1188 Cretaceous (Lower Albian) Escucha Formation of northeastern Spain. *PLoS One*
1189 **8**:e80405. DOI: https://doi.org/10.1371/journal.pone.0080405

1190 Kvaček J, Barrón E, Heřmanová Z, Mendes MM, Karch J, Žemlička J, Dudák J. 2018.
1191 Araucarian conifer from late Albian amber of northern Spain. *Papers in*
1192 *Palaeontology* **4**:643–656. DOI: https://doi.org/10.1002/spp2.1223
1193 Langenheim JH. 1967. Preliminary investigations of *Hymenaea courbaril* as a resin
1194 producer. *Journal of the Arnold Arboretum* **48**:203–230.
1195 Langenheim JH. 2003. *Plant Resins: Chemistry, Evolution, Ecology, and*
1196 *Ethnobotany*. Portland, USA: Timber Press.
1197 Levings SC, Windsor DM. 1985. Litter arthropod populations in a tropical deciduous
1198 forest: relationships between years and arthropod groups. *The Journal of Animal*
1199 *Ecology* **54**:61–69. DOI: https://doi.org/10.2307/4620
1200 Lozano RP, Pérez-de la Fuente R, Barrón E, Rodrigo A, Viejo JL, Peñalver E. 2020.
1201 Phloem sap in Cretaceous ambers as abundant double emulsions preserving
1202 organic and inorganic residues. *Scientific Reports* **10**:9751. DOI:
1203 https://doi.org/10.1038/s41598-020-66631-4
1204 Martin JH, Mifsud D, Rapisarda C. 2000. The whiteflies (Hemiptera: Aleyrodidae) of
1205 Europe and the Mediterranean basin. Bulletin Entomological Research **90**:407–
1206 448. DOI: https://doi.org/10.1017/S0007485300000547
1207 Martín-Closas C. 2000. *Els caròfits del Juràssic superior i Cretaci Inferior de la*
1208 *Península Ibèrica*. Barcelona, Spain: Institut d'Estudis Catalans, Arxius de les
1209 Seccions de Ciències, vol. 125.
1210 Martín-Closas C, Vicente A, Pérez-Cano J, Sanjuan J., Bover-Arnal, T. 2018. On the
1211 earliest occurrence of *Tolypella* section *Tolypella* in the fossil record and the age
1212 of major clades in extant Characeae. *Botany Letters* **165**:23–33. DOI:
1213 https://doi.org/10.1080/23818107.2017.1387078

1214 Martínez-Delclòs X, Briggs DE, Peñalver E. 2004. Taphonomy of insects in
1215 carbonates and amber. *Palaeogeography, Palaeoclimatology, Palaeoecology*
1216 **203**:19–64. DOI: https://doi.org/10.1016/S0031-0182(03)00643-6
1217 McAlpine JF, Peterson BV, Shewell GE, Teskey HJ, Vockeroth JR, Wood DM. 1981.
1218 Manual of Nearctic Diptera. Ottawa, Canada: Research Branch Agriculture
1219 Canada.
1220 McDonald AT, Espílez E, Mampel L, Kirkland JI, Alcalá L. 2012. An unusual new
1221 basal iguanodont (Dinosauria: Ornithopoda) from the Lower Cretaceous of Teruel,
1222 Spain. *Zootaxa* **3595**:61–76. DOI: https://doi.org/10.11646/zootaxa.3595.1.3
1223 McKellar RC, Jones E, Engel MS, Tappert R, Wolfe AP, Muehlenbachs K, Cockx P,
1224 Koppelhus EB, Currie, PJ. 2019. A direct association between amber and dinosaur
1225 remains provides paleoecological insights. *Scientific Reports* **9**:17916. DOI:
1226 https://doi.org/10.1038/s41598-019-54400-x
1227 Meléndez A, Soria AR, Meléndez N. 2000. A coastal lacustrine system in the Lower
1228 Barremian from the Oliete Sub-basin, central Iberian Range, northeastern Spain.
1229 In: Gierlowski-Kordesch EH, Kelts KR (Eds), *Lake Basins Through Space and*
1230 *Time*. Tulsa, USA: The American Association of Petroleum Geologists, Studies in
1231 Geology 46, pp. 279–284.
1232 Menor-Salván C, Simoneit BRT, Ruiz-Bermejo M, Alonso J. 2016. The molecular
1233 composition of Cretaceous ambers: Identification and chemosystematic relevance
1234 of 1,6-dimethyl-5-alkyltetralins and related bisnorlabdane biomarkers. *Organic*
1235 *Geochemistry* **93**:7–21. DOI: https://doi.org/10.1016/j.orggeochem.2015.12.010
1236 Najarro M, Peñalver E, Rosales I, Pérez-de la Fuente R, Daviero-Gomez V, Gomez
1237 B, Delclòs X. 2009. Unusual concentration of Early Albian arthropod-bearing
1238 amber in the Basque-Cantabrian Basin (El Soplao, Cantabria, Northern Spain):

palaeoenvironmental and palaeobiological implications. *Geologica Acta* **7**:363–387. DOI: https://doi.org/10.1344/105.000001443

Najarro M, Peñalver E, Pérez-de la Fuente R, Ortega-Blanco J, Menor-Salván C, Barrón E, Soriano C, Rosales I, López Del Valle R, Velasco F, Tornos F, Daviero-Gomez V, Gomez B, Delclòs X. 2010. Review of the El Soplao amber outcrop, Early Cretaceous of Cantabria, Spain. *Acta Geologica Sinica (English Edition)* **84**:959–976. DOI: https://doi.org/10.1111/j.1755-6724.2010.00258.x

Nel A, DePalma RA, Engel MS. 2010. A possible hemiphlebiid damselfly in Late Cretaceous amber from South Dakota (Odonata: Zygoptera). *Transactions of the Kansas Academy of Science* **113**:231–234.

Néraudeau D, Perrichot V, Dejax J, Masure E, Nel A, Phillipe M, Moreau P, Guillocheau F, Guyot T. 2002. A new fossil locality with insects in amber and plants (likely Uppermost Albian): Archingeay (Charente-Maritime, France). *Geobios* **35**:233–240. DOI: https://doi.org/10.1016/S0016-6995(02)00024-4

Néraudeau D, Allain R, Perrichot V, Videt B, de Lapparent de Broin F, Guillocheau F, Philippe M, Rage J-C, Vullo, R. 2003. Découverte d'un dépôt paralique à bois fossiles, ambre insectifère et restes d'Iguanodontidae (Dinosauria, Ornithopoda) dans le Cénomanien inférieur de Fouras (Charente-Maritime, Sud-Ouest de la France). *Comptes Rendus Palevol* **2**:221–230. DOI: https://doi.org/10.1016/S1631-0683(03)00032-0

Ortega-Blanco J, Peñalver E, Delclòs X, Engel MS. 2011. False fairy wasps in early Cretaceous amber from Spain (Hymenoptera: Mymarommatoidea). *Palaeontology* **54**:511–523. DOI: https://doi.org/10.1111/j.1475-4983.2011.01049.x

1262 Ortega-Blanco J, McKellar RC, Engel MS. 2014. Diverse scelionid wasps from Early
1263 Cretaceous Álava amber, Spain (Hymenoptera: Platygastroidea). *Bulletin of*
1264 *Geosciences* **89**:553–571. DOI: https://doi.org/10.3140/bull.geosci.1463
1265 Peñalver E, Delclòs X. 2010. Spanish amber. In: Penney D (Ed), *Biodiversity of*
1266 *Fossils in Amber from the Major World Deposits*. Rochdale, UK: Siri Scientific
1267 Press, pp. 236–270.
1268 Peñalver E, Delclòs X, Soriano C. 2007. A new rich amber outcrop with
1269 palaeobiological inclusions in the Lower Cretaceous of Spain. *Cretaceous*
1270 *Research* **28**:791–802. DOI: https://doi.org/10.1016/j.cretres.2006.12.004
1271 Peñalver E, González-Fernández B, López Del Valle R, Barrón E, Lozano RP,
1272 Rodrigo A, Pérez-de la Fuente R, Menéndez-Casares E, Sarto i Monteys V. 2018.
1273 Un nuevo yacimiento de ámbar cretácico en Asturias (norte de España):
1274 Resultados preliminares de la excavación paleontológica de 2017 en La Rodada
1275 (La Manjoya). In: Vaz N, Sá AA (Eds), *Yacimientos Paleontológicos*
1276 *Excepcionales en la Península Ibérica*. Madrid, Spain: Instituto Geológico y Minero
1277 de España, Cuadernos del Museo Geominero, 27, pp. 289–299.
1278 Pérez-Cano J, Bover-Arnal T, Martín-Closas C. 2020. Barremian charophytes from
1279 the Maestrat Basin. *Cretaceous Research* **115**:104544. DOI:
1280 https://doi.org/10.1016/j.cretres.2020.104544
1281 Pérez-de la Fuente R, Delclòs X, Peñalver E, Arillo A. 2011. Biting midges (Diptera:
1282 Ceratopogonidae) from the Early Cretaceous El Soplao amber (N Spain).
1283 *Cretaceous Research* **32**:750–761. DOI:
1284 https://doi.org/10.1016/j.cretres.2011.05.003
1285 Pérez-García A, Espílez E, Mampel L, Alcalá L. 2015. A new European Albian turtle
1286 that extends the known stratigraphic range of the Pleurosternidae

(Paracryptodira). *Cretaceous Research* **55**:74–83. DOI: https://doi.org/10.1016/j.cretres.2015.02.007

Pérez-García A, Espílez E, Mampel L, Alcalá L. 2020. A new basal turtle represented by the two most complete skeletons of Helochelydridae in Europe. *Cretaceous Research* **107**:104291. DOI: https://doi.org/10.1016/j.cretres.2019.104291

Peris D. 2020. Coleoptera in amber from Cretaceous resiniferous forests. *Cretaceous Reseach* **113**:104484. DOI: https://doi.org/10.1016/j.cretres.2020.104484

Peris D, Labandeira CC, Barrón E, Delclòs X, Rust J, Wang B. 2020. Generalist pollen-feeding beetles during the mid-Cretaceous. *iScience* **23**:100913. DOI: https://doi.org/10.1016/j.isci.2020.100913

Perrichot V, Néraudeau D, Nel A, De Ploeg G. 2007. A reassessment of the Cretaceous amber deposits from France and their palaeontological significance. *African Invertebrates* **48**:213–227.

Perrichot V, Néraudeau D, Tafforeau P. 2010. Charentese amber. In: Penney D (Ed), *Biodiversity of Fossils in Amber from the Major World Deposits*. Rochdale, UK: Siri Scientific Press, pp. 193–208.

Peyrot D, Rodríguez-López JP, Barrón E, Meléndez N. 2007. Palynology and biostratigraphy of the Escucha Formation in the Early Cretaceous Oliete Sub-basin, Teruel, Spain. *Revista Española de Micropaleontología* **39**:135–154.

Poinar G, Lambert JB, Wu Y. 2007. Araucarian source of fossiliferous Burmese amber: spectroscopic and anatomical evidence. *Journal of the Botanical Research Institute of Texas* **1**:449–455.

Rasnitsyn AP, Quicke DL. 2002. *History of insects*. Amsterdam, Netherlands: Kluwer Academic Publishers.

1311 Rodríguez-López JP, Meléndez N, Soria AR, De Boer PL. 2009. Reinterpretación
1312 estratigráfica y sedimentológica de las formaciones Escucha y Utrillas de la
1313 Cordillera Ibérica. *Revista de la Sociedad Geológica de España* **22**:163–219.
1314 Riveline J, Berger J-P, Feist M, Martín-Closas C, Schudack M, Soulié-Märsche I.
1315 1996. European Mesozoic-Cenozoic charophyte biozonation. *Bulletin de la*
1316 *Société Géologique de France* **167**:453–468.
1317 Rogers RR, Eberth DA, Fiorillo AR. 2007. *Bonebeds. Genesis, Analysis and*
1318 *Paleobiological Significance*. Chicago, USA: The University of Chicago Press.
1319 Salas R, Guimerà J. 1996. Rasgos estructurales principales de la cuenca cretácica
1320 inferior del Maestrazgo (Cordillera Ibérica oriental). *Geogaceta* **20**:1704–1706.
1321 Sames B. 2011. Early Cretaceous *Theriosynoecum* Branson 1936 in North America
1322 and Europe. *Micropaleontology* **57**:291–344.
1323 Schmidt AR, Jancke S, Lindquist EE, Ragazzi E, Roghi G, Nascimbene PC, Schmidt
1324 K, Wappler T, Grimaldi D. 2012. Arthropods in amber from the Triassic Period.
1325 *Proceedings of the National Academy of Science of the United States of America*
1326 **109**:14796–14801. DOI: https://doi.org/10.1073/pnas.1208464109
1327 Seyfullah LJ, Beimforde C, Dal Corso J, Perrichot V, Rikkinen J, Schmidt AR. 2018.
1328 Production and preservation of resins – past and present. *Biological Reviews*
1329 **93**:1684–1714. DOI: https://doi.org/10.1111/brv.12414
1330 Seyfullah LJ, Roberts EA, Schmidt AR, Ragazzi E, Anderson KB, Rodrigues do
1331 Nascimento Jr D, Ferreira da Silva Filho W, Kunzmann L. 2020. Revealing the
1332 diversity of amber source plants from the Early Cretaceous Crato Formation,
1333 Brazil. *BMC Evolutionary Biology* **20**:107. DOI: https://doi.org/10.1186/s12862-020-
1334 01651-2

1335 Speranza M, Ascaso C, Delclòs X, Peñalver E. 2015. Cretaceous mycelia preserving
1336 fungal polysaccharides: Taphonomic and paleoecological potential of
1337 microorganisms preserved in fossil resins. *Geologica Acta* **13**:363–385. DOI:
1338 https://doi.org/10.1344/GeologicaActa2015.13.4.8
1339 Strachan MG, Alexander R, Kagi RI. 1988. Trimethylnaphthalenes in crude oils and
1340 sediments: Effects of source and maturity. *Geochimica et Cosmochimica Acta*
1341 **52**:1255–1264. DOI: https://doi.org/10.1016/0016-7037(88)90279-7
1342 Stuchlik L, Ziembińska-Tworzydło M, Kohlman-Adamska A, Grabowska I, Ważyńska
1343 H, Sadowska A. 2002. *Atlas of Pollen and Spores of the Polish Neogene Vol. 2,*
1344 *Gymnosperms*. Warsaw, Poland: Polish Academy of Sciences.
1345 Tanke DH. 2004. Mosquitoes and mud: The 2003 Royal Tyrrell Museum of
1346 Palaeontology expedition to the Grande Praire region (Northwestern Alberta,
1347 Canada). *Alberta Paleontological Society Bulletin* **19**:3–31.
1348 Tanrikulu S, Doyle JA, Delusina I. 2018. Early Cretaceous (Albian) spores and pollen
1349 from the Glen Rose Formation of Texas and their significance for correlation of the
1350 Potomac Group. *Palynology* **42**:438–456. DOI:
1351 https://doi.org/10.1080/01916122.2017.1374309
1352 Taylor TN, Alvin KL. 1984. Ultrastructure and development of Mesozoic pollen:
1353 *Classopollis*. *American Journal of Botany* **71**:575–587.
1354 Taylor DW, Hu S. 2010. Coevolution of early angiosperms and their pollinators:
1355 Evidence for pollen. *Palaeontographica Abteilung B* **283**:103–135. DOI:
1356 https://doi.org/10.1127/palb/283/2010/103
1357 Tibert NE, Colin JP, Kirkland JI, Alcalá L, Martín-Closas C. 2013. Lower Cretaceous
1358 nonmarine ostracodes from an Escucha Formation dinosaur bonebed in eastern
1359 Spain. *Micropaleontology* **59**:83–91.

Tihelka E, Huang D, Perrichot V, Cai C. 2021. A previously missing link in the evolution of dasytine soft-winged flower beetles from Cretaceous Charentese amber (Coleoptera, Melyridae). *Papers in Palaeontology*, 12 pp. DOI: https://doi.org/10.1002/spp2.1360

Trabelsi K, Sames B, Nasri A, Piovesan EK, Elferhi F, Skanji A, Houla Y, Soussi M, Wagreich M. 2021. Ostracods as proxies for marginal marine to non-marine intervals in the mid-Cretaceous carbonate platform of the Central Tunisian Atlas (North Africa): Response to major short-term sea-level falls. *Cretaceous Research* **117**:104581. DOI: https://doi.org/10.1016/j.cretres.2020.104581

Traverse A. 2007. *Paleopalynology*. Dordrecht, Netherlands: Springer, 2nd Edition.

Vajda V, Pesquero Fernández MD, Villanueva-Amadoz U, Lehsten V, Alcalá L. 2016. Dietary and environmental implications of Early Cretaceous predatory dinosaur coprolites from Teruel, Spain. *Palaeogeography, Palaeoclimatology, Palaeoecology* **464**:134–142. DOI: https://doi.org/10.1016/j.palaeo.2016.02.036

Van Konijnenburg-Van Cittert JHA. 2002. Ecology of some Late Triassic to Early Cretaceous ferns in Eurasia. *Review of Palaeobotany and Palynology* **119**:113–124. DOI: https://doi.org/10.1016/S0034-6667(01)00132-4

Vance TC. 1974. Larvae of the Sericothripini (Thysanoptera: Thripidae), with reference to other larvae of the Terebrantia, of Illinois. *Illinois Natural History Survey Bulletin* **31**:144–208.

Villanueva-Amadoz U, Sender LM, Alcalá L, Pons D, Royo-Torres R, Diez JB. 2015. Paleoenvironmental reconstruction of an Albian plant community from the Ariño bonebed layer (Iberian Chain, NE Spain). *Historical Biology* **27**:430–441. DOI: https://doi.org/10.1080/08912963.2014.895826

1384 Zheng D, Chang S-C, Perrichot V, Dutta S, Rudra A, Mu L, Kelly RS, Zhang Qi,
1385 Zhang Qin, Wong J, Wang J, Wang H, Fang Y, Zhang H, Wang B. 2018. A Late
1386 Cretaceous amber biota from central Myanmar. *Nature Communications* **9**:3170.
1387 DOI: https://doi.org/10.1038/s41467-018-05650-2